ACR No. 3F11

NATIONAL ADVISORY COMMITTEE FOR AERONAUTICS

WARTIME REPORT

ORIGINALLY ISSUED
June 1943 as
Advance Confidential Report 3F11

WIND-TUNNEL TESTS OF AILERONS AT VARIOUS SPEEDS

I - AILERONS OF 0.20 AIRFOIL CHORD AND TRUE CONTOUR WITH 0.35 AILERON-CHORD EXTREME BLUNT NOSE BALANCE ON THE NACA 66,2-216 AIRFOIL

By W. Letko, H. G. Denaci, and C. Freed

Langley Memorial Aeronautical Laboratory
Langley Field, Va.

1.2.1.2
1.2.1.5.1
1.8.2.2
1.8.2.5

NACA

WASHINGTON

L - 431

NATIONAL ADVISORY COMMITTEE FOR AERONAUTICS

ADVANCE CONFIDENTIAL REPORT

WIND-TUNNEL TESTS OF AILERONS AT VARIOUS SPEEDS

I - AILERONS OF 0.20 AIRFOIL CHORD AND TRUE CONTOUR WITH 0.35 AILERON-CHORD EXTREME BLUNT NOSE BALANCE ON THE NACA 66,2-216 AIRFOIL

By W. Letko, H. G. Denaci, and C. Freed

SUMMARY

Hinge-moment, lift, and pressure-distribution measurements were made in the two-dimensional test section of the NACA stability tunnel on a blunt-nose balance-type aileron on an NACA 66,2-216 airfoil at speeds up to 360 miles per hour corresponding to a Mach number of 0.475. The tests were made primarily to determine the effect of speed on the action of this type of aileron. The balance-nose radii of the aileron were varied from 0 to 0.02 of the airfoil chord and the gap width was varied from 0.0005 to 0.0107 of the airfoil chord. Tests were also made with the gap sealed.

The variations in hinge moments and lift with Mach number, angle of attack, and aileron deflection are given in the form of curves of section hinge-moment coefficients and section lift coefficients plotted against aileron deflection for the various conditions tested, together with cross plots showing the general effect of Mach number, gap width, and balance-nose radii.

The results show that there was a considerable increase in the stalled range of the aileron with increased speed. Up to the stall, the variation in hinge-moment coefficients and lift coefficients for the speed range tested was small but the variation may be appreciable when stick forces at high speeds are considered.

INTRODUCTION

Large increases in the size and speeds of current combat airplanes, in addition to high maneuverability required in combat, have made it necessary to balance almost exactly the hinge moments of ailerons and at the same time to maintain their effectiveness. Although most types of aileron balances in use today operate satisfactorily at low speeds, difficulty, such as overbalance at high speeds, has been experienced with some existing aileron installations. This difficulty is apparently caused by the large amount of balance coupled with the changes in hinge moment that result from compressibility effects. Consideration of these problems has made necessary further research on some of the currently used or recently proposed balance arrangements.

The NACA is therefore undertaking a study of some of the more promising aileron types at higher Mach numbers than were employed in previous developments. This report deals with the section characteristics of a blunt-nose balance type of aileron of 0.20 airfoil chord with a 0.35 aileron balance and of true contour used on an NACA 66,2-216 airfoil. The amount of balance, 0.35 aileron chord, was chosen because, from the data given in reference 1, it was estimated that this amount of balance would give almost complete balance on an airfoil of the NACA 230 series at a low angle of attack.

The section lift coefficient c_l and the section hinge-moment coefficient c_{h_a} were measured at various airspeeds up to 360 miles per hour, corresponding to a Mach number of 0.475. These measurements were taken through an angle-of-attack range from -5° to 10° and an aileron deflection range of $\pm 20^\circ$. The influence of the gap width between the aileron and wing and the influence of the radii of the projecting corners of the balance were investigated. The data are presented in the form of curves of c_l and c_{h_a} plotted against aileron deflection with cross plots to show the effect of the aileron parameters.

SYMBOLS

c_l airfoil section lift coefficient $\left(\frac{l}{qc}\right)$

Δc_l increment of airfoil section lift coefficient

L-431

$c_{m_{c/4}}$ airfoil section pitching-moment coefficient about quarter-chord point of airfoil $\left(\frac{m_{c/4}}{qc^2}\right)$

c_{h_a} aileron section hinge-moment coefficient $\left(\frac{h_a}{qc_a^2}\right)$

l airfoil section lift

$m_{c/4}$ airfoil section pitching moment about quarter-chord point of airfoil

h_a aileron section hinge moment

c chord of basic airfoil, including aileron

c_a chord of aileron measured from hinge axis back to trailing edge

q dynamic pressure $\left(\frac{1}{2}\rho V^2\right)$

V air velocity

ρ mass density of air

α_o angle of attack for airfoil of infinite aspect ratio

δ_a aileron deflection with respect to airfoil

M Mach number

APPARATUS AND MODELS

The tests were made in the two-dimensional test section of the stability tunnel at airspeeds up to 360 miles per hour. The test section is rectangular, 2.5 feet wide and 6 feet high.

The model of an NACA 66,2-216, a = 1.0 section was made of laminated mahogany. It completely spanned the test section and was fixed into circular end disks that were flush with the tunnel walls. The angle of attack of the model was changed by rotating the end disks. Tables I and II give the ordinates of the airfoil section and locations of centers of balance-nose radii, respectively. Figure 1 is a photograph of a model mounted in the tunnel.

The aileron of 0.20c and $0.35c_a$ balance and of true contour was made of steel with wooden nose pieces having 0, 0.01c, and 0.02c balance-nose radii. (See fig. 2.) The aileron was supported at the ends by ball bearings mounted in steel end plates attached to the airfoil.

The aileron deflection was varied and the aileron angle and hinge moments were measured by a calibrated spring torque balance and sector system. Pressure orifices were located along the midspan of the wing and aileron and the pressure distribution was recorded photographically. In some cases hinge moments and lift were obtained from the pressure-distribution diagrams.

For some of the tests the lift was also measured by an integrating manometer connected to orifices in the floor and ceiling of the tunnel. The integrating manometer was calibrated against lift obtained by pressure distribution.

TESTS

Tests were made with balance-nose radii of 0, 0.01c, and 0.02c. With zero radii only pressure-distribution tests were made. With radii of 0.01c and 0.02c, hinge moments were measured with gap widths of 0.0005c, 0.0030c, 0.0055c, and 0.0107c and also with a 0.0055c gap sealed with a flexible sheet that extended from wall to wall. In the test in which the 0.02c radii was used - in addition to the pressure-distribution and hinge-moment measurements - section lift was measured by the integrating manometer.

Tests for each condition were made at five speeds which gave Mach numbers in a range between 0,195 and 0.475. The lowest speed corresponds to a Reynolds number of about 2,800,000 and the highest speed to a Reynolds number of about 6,700,000. Figure 3 is a plot of Reynolds number based on standard atmospheric conditions against test Mach number. Tests were made at angles of attack of -5°, 0°, 5°, and 10° with -2°, 2°, and 7.5° added for the 0.0055c gap (open and sealed). For each angle of attack readings were taken at the following aileron angles: 0, $\pm 2^\circ$, $\pm 5^\circ$, $\pm 7^\circ$, $\pm 10^\circ$, $\pm 13^\circ$, $\pm 16^\circ$, $\pm 18^\circ$, and $\pm 20^\circ$.

The high speeds could not be attained at the large angles of attack with large aileron deflections because of limited tunnel power.

Pressure-distribution records were taken at Mach numbers of 0.195, 0.358, and 0.475 for every angle of attack tested. For each angle of attack records were made at aileron angles of 0, ±5°, -7°, ±10°, and ±16°.

PRECISION

Angles of attack were set to within ±0.1° and aileron angles to within ±0.3°. The hinge-moment coefficients that were measured could be repeated to within ±0.003 and the lift coefficients to within ±0.01.

Corrections for tunnel-wall effects were not applied to the section hinge-moment coefficients. The following corrections were applied to the section lift and section pitching-moment coefficients and to the angle of attack:

$$c_l = [1 - \Upsilon (1 + 2\beta)]\, c_l'$$

$$c_{m_{c/4}} = (1 - 2\beta\Upsilon)\, c_{m_{c/4}}' + \frac{\Upsilon c_l'}{4}$$

$$\alpha_0 = (1 + \Upsilon)\alpha'$$

where

$$\Upsilon = \frac{\pi^2}{48}\left(\frac{c}{h}\right)^2$$

h height of tunnel

β = 0.304 (theoretical factor for NACA 66,2-216, a = 1 airfoil)

c_l' measured lift coefficient

$c_{m_{c/4}}'$ measured pitching-moment coefficient

α' uncorrected or geometric angle of attack

The values used are:

$$c_l = 0.963\ c_l'$$

$$c_{m_{c/4}} = 0.986\ c_{m_{c/4}} + 0.006\ c_l'$$

$$\alpha_o = 1.023\ \alpha'$$

Hinge moments were measured simultaneously by pressure distribution and by the spring torque balance for a number of varied conditions and the results are shown in figure 4. The variation in the values is probably due to the fact that the spring balance measures the hinge moment on the entire aileron, which includes effects of boundary layer at the tunnel wall and of gaps at the ends of the aileron as well as the effects of any cross flow over the aileron; whereas the pressure distribution gives the hinge moment at one section of the aileron and is subject to some errors in fairing the pressure-distribution diagrams.

RESULTS AND DISCUSSION

In order that the results for the tests of various model configurations may be more easily found table III gives the figure numbers, the variations shown on the figure, and the corresponding model configuration. Only part of the data are presented for the 0 and 0.01c balance-nose radii.

The results show that for all conditions the aileron apparently stalled at an angle of deflection that depended on the speed, the angle of attack, the gap width, and the balance-nose radii and that the hinge moments increased rapidly in the stalled range. At the transition point between the stalled and unstalled range the aileron was observed to oscillate between the stalled and unstalled condition. As the speed increased the unstalled range of deflections of the aileron generally became smaller. The effect was most pronounced with the zero balance-nose radii.

Hinge Moment of Aileron

The aileron section hinge-moment coefficients c_{h_a} plotted against aileron deflection δ_a are given in figures 5 to 7. The values of c_{h_a} given in figure 5 are

L-431

from pressure-distribution records (no other satisfactory measurements were available); those given in figures 6 and 7 are from spring-balance measurements (a comparison of results obtained by the two methods is given in figure 4). These results show that for a limited range of aileron deflections and angles of attack the aileron balance was fairly effective. An average value of the slope of the curve of section hinge-moment coefficient plotted against aileron angle, $\frac{\partial c_{h_a}}{\partial \delta_a}$, of -0.0057 was obtained from values of c_{h_a} at a δ_a of $\pm 5^\circ$ as compared to a value of -0.011 given by unpublished data for a 0.20 chord plain sealed aileron on the same wing section. Although the value of $\frac{\partial c_{h_a}}{\partial \delta_a}$ of -0.0057 is relatively large for combat airplanes, the increment reduction in the value of $\frac{\partial c_{h_a}}{\partial \delta_a}$ is, according to data reported in reference 1, about the same as would be obtained for a $0.35c_a$ balance aileron on an NACA 230-series section.

For the range of Mach numbers M tested the most noticeable effect of increasing speed on the hinge-moment characteristics of the ailerons was a considerable increase in the stalled range of the aileron. The general trend of the effect of M on c_{h_a} in the unstalled deflection range is shown by figure 8 to be an increase in c_{h_a} with increase of M. Some of this trend may be due to the change in Reynolds number. Approximate values of Reynolds number for any value of M may be obtained from figure 3.

A change in the unstalled range of the aileron is shown by figures 5 to 7 to be the principal effect on the hinge-moment characteristics resulting from changes in balance-nose radii and gap width. An increase in radii from 0 to 0.02c changed the unstalled range from about $\pm 4^\circ$ to about $\pm 10^\circ$ and increased the hinge-moment-coefficient slope. For all cases, the aileron with gap sealed had the greatest unstalled range. An increase in the gap decreased appreciably the unstalled range; the amount of change varied with angle of attack and the effect was usually greater for the positive range of aileron deflections than for the negative range.

Figure 9 shows that the effect of gap on c_{h_a} in the unstalled range is usually small. The general variation of c_{h_a} with α_0 is shown in figure 10. Here again the effects of M, balance-nose radii, and gap are small.

Lift

The airfoil section lift curves, c_l (obtained with the integrating manometer) for a balance-nose radii of 0.02c with aileron neutral, are presented in figure 11 and show that the slope of the lift curve increases with Mach number. The variation of lift-curve slope with speed for the various gap widths is given in figure 12 together with a curve showing the theoretical variation. It is believed that closer agreement would have been obtained if the compressibility effect on tunnel-wall interference and Reynolds number effects on the airfoil characteristics had been taken into account. Figure 12 also shows that the highest slopes were obtained with the gap sealed. When the gap was unsealed, an increase in the gap width caused a decrease in the slope except at the highest speed tested where an increase in gap resulted in an increase in the slope.

Figure 13 is a plot of section lift coefficient against aileron angle. In order to avoid confusion, faired curves have been drawn in this figure only through the test points for a Mach number of approximately 0.36. For low and medium angles of attack an increase in the speed increases the value of the slope of these curves $\left(\frac{\partial c_l}{\partial \delta_a}\right)_\alpha$ and the amount of increase varies with the angle of attack. At high angles of attack an increase in speed generally caused a decrease in the value of $\left(\frac{\partial c_l}{\partial \delta_a}\right)_\alpha$.

Figure 13 also shows that the value of $\left(\frac{\partial c_l}{\partial \delta_a}\right)_\alpha$, for a range of δ_a of ±5, was highest at low and medium angles of attack with the gap sealed and, at high angles of attack, the slope was highest for the 0.0055c gap. Increases in gap usually decreased the aileron deflection at which the stall occurred and decreased considerably the effectiveness of the aileron at large aileron deflections. The loss in

L-431

effectiveness due to the gap at large aileron deflections was least at the high speeds.

The airfoil section lift and section pitching-moment coefficients obtained by pressure distribution for balance-nose radii of 0 and 0.02c are presented in figure 14. Figure 14(a) shows, as might be expected, that there is little change in the lift curve (aileron neutral) with changes in balance-nose radii. Figure 14(b) shows the variation of the airfoil section lift coefficient c_l with aileron deflection for the different radii. It is evident that the aileron with 0.02c radii has a much larger effective range than either of the other two ailerons and that the aileron with zero radii is inefficient because it loses all its effectiveness at a positive aileron deflection of 5°.

Variations of airfoil section lift coefficient c_l with Mach number for balance-nose radii of 0.02c are shown in figure 15 for three aileron deflections. The general tendency, as expected, is for the lift coefficient to increase with Mach number; part of this increase probably is due to Reynolds number. At an angle of attack of 10°, however, the lift coefficient decreased after a certain value of Mach number was reached as a result of critical speed occurring over the leading edge of the airfoil.

Increasing the gap width from 0.0005c to 0.0107c generally caused a slight decrease in the value of c_l. (See fig. 16.) The aileron with 0.02c balance-nose radii used in this test is somewhat more effective in producing lift at an angle of attack of 10° than a plain sealed flap of 0.20c on the same type airfoil at approximately the same Reynolds number, as is indicated by the data given in reference 2.

Control-Force Criterion

The variation of $\Delta c_{h_a}\delta_a$ with Δc_l is a control-force criterion that takes into account not only the reduction in Δc_{h_a} but also the possible reduction in Δc_l (for a given deflection) that may be caused by the balancing device. Therefore, even though Δc_{h_a} may be reduced considerably, if it is necessary to move the control surface through a very large angle (decreasing the stick leverage of the ailerons) the product may be increased somewhat to obtain the same Δc_l. The criterion as used herein is strictly valid only at the instant that the aileron is deflected. The use of this criterion for computing stick forces during a roll will give an erroneous indication of these forces because differences in the rates of variation of hinge-moment coefficients with angle of attack $(\partial c_h/\partial \alpha)$ of the ailerons that are being compared are not taken into account.

Figure 17, a plot of $\Delta c_{h_a}\delta_a$ against Δc_l for various Mach numbers, shows that the effect of Mach number on the balance effectiveness is small except for high aileron deflections. Generally there is a decrease in the range of balance effectiveness with speed. In some cases, however, the effective range increases with small changes of speed but is decreased with further increases in speed.

Figure 18 shows the variation of $\Delta c_{h_a}\delta_a$ with Δc_l for the different balance-nose radii. The effective lift-producing range is very small for the zero radii and is greatest for the 0.02c radii.

Figure 19 shows the variation of $\Delta c_{h_a}\delta_a$ with Δc_l for the various gap widths. For small and negative angles of attack the results were best with gap sealed but at higher angles the results were best with a gap width of 0.0055c.

A plot to show the variation of $\Delta c_{h_a}\delta_a$ with Δc_l for various angles of attack (fig. 20) has been included as a matter of interest and, also, for possible comparisons with other ailerons.

The results of these tests indicate that a greater amount of balance than that used in this investigation is necessary if the ailerons are to give satisfactory hinge moments for use on combat airplanes. The range of balance effectiveness and the range for which the aileron is effective in producing rolling moments could probably be extended by an increase in the balance-nose radii.

For the range of speeds tested, increases in speed caused a considerable increase in the stalled range of the aileron and in the unstalled range there were small increases in the hinge moments. Higher speeds, however, probably would have more effect because it is usually not until higher speeds are reached that the lift and drag characteristics of airfoils are seriously affected by compressibility.

L-431

CONCLUSIONS

The results of the tests of ailerons of 0.20 airfoil chord and true contour with 0.35 aileron-chord extreme blunt nose balance on the NACA 66,2-216 airfoil indicate the following general conclusions:

1. Increasing the Mach number up to 0.470 generally causes a small increase of the hinge-moment and lift coefficients but increases the stalled range of the ailerons considerably.

2. An increase of the balance-nose radii from 0 to 0.02 chord increases the range for which the aileron is effective by about 8° but results in increased hinge-moment coefficients with little change in lift coefficients in the unstalled range.

3. An increase of the gap width increased the hinge-moment coefficients slightly with little change in lift coefficient; however, a considerable increase in the stalled range of the aileron results. The magnitude of the increase varies with the angle of attack.

4. The amount of balance tested, 0.35 aileron chord, gave no case of complete balance and in some cases the unbalance was relatively large.

Langley Memorial Aeronautical Laboratory,
National Advisory Committee for Aeronautics,
Langley Field, Va.

REFERENCES

1. Purser, Paul E., and Toll, Thomas A.: Wind-Tunnel Investigation of the Characteristics of Blunt-Nose Ailerons on a Tapered Wing. NACA A.R.R., Feb. 1943.

2. Jacobs, Eastman N., Abbott, Ira H., and Davidson, Milton: Supplement to NACA Advance Confidential Report, Preliminary Low-Drag-Airfoil and Flap Data from Tests at Large Reynolds Numbers and Low Turbulence. NACA, (Loose leaf), March 1942.

TABLE I. - ORDINATES FOR NACA 66,2-216, a = 1.0 AIRFOIL

[Stations and ordinates in percent of wing chord]

Upper surface		Lower surface	
Station	Ordinate	Station	Ordinate
0	0	0	0
.401	1.230	.599	-1.130
.640	1.484	.860	-1.344
1.128	1.858	1.372	-1.644
2.362	2.560	2.638	-2.188
4.846	3.604	5.154	-2.972
7.340	4.428	7.660	-3.580
9.838	5.140	10.162	-4.106
14.845	6.276	15.155	-4.930
19.860	7.156	20.140	-5.564
24.879	7.844	25.121	-6.054
29.900	8.366	30.100	-6.422
34.924	8.736	35.076	-6.676
39.949	8.980	40.051	-6.838
44.974	9.092	45.026	-6.902
50.000	9.060	50.000	-6.854
55.025	8.875	54.975	-6.685
60.048	8.496	59.952	-6.354
65.067	7.862	64.933	-5.802
70.081	6.941	69.919	-4.997
75.087	5.860	74.913	-4.070
80.085	4.644	79.915	-3.052
85.075	3.395	84.925	-2.049
90.055	2.103	89.945	-1.069
95.028	.913	94.972	-.281
100.000	0	100.000	0
L.E. radius: 1.575			

TABLE II. - LOCATION OF CENTERS OF BALANCE-NOSE RADII

[Stations and ordinates in percent of wing chord]

Balance-nose radii	Upper surface		Lower surface	
	Station	Ordinate	Station	Ordinate
0	75.17	5.83	75.00	-4.04
1	75.50	4.75	75.33	-2.96
2	75.87	3.62	75.79	-1.83

Figure	Variation shown	Balance-nose radii	Gap width
5	ch_a against δ_a (by pressure distribution)	0c	0.0055c
6	ch_a against δ_a	.01c	.0055c
7	ch_a against δ_a	.02c	(a) .0005c (b) .0030c (c) .0055c (d) .0107c (e) .0055c (sealed)
8	ch_a against M	(a) .01c (b) .02c	.0055c .0055c (sealed)
9	ch_a against gap	(a) .01c (b) .02c	Varies
10	ch_a against α_o	(a) .01c (b) .02c	0.0055c .0055c (sealed)
11	c_l against α_o	.02c	.0005c .0055c .0107c .0055c (sealed)
12	$\left(\frac{\partial c_l}{\partial \alpha}\right)_{\delta_a=0}$ against M	.02c	.0005c .0055c .0107c .0055c (sealed)
13	c_l against δ_a	.02c	(a) .0005c (b) .0055c (c) .0107c (d) .0055c (sealed)
14	c_l and $c_{m_{c/4}}$ obtained by pressure distribution (a) Variation with α_o (b) Variation with δ_a	0c .01c .02c	.0055c
15	c_l against M	.02c	.0055c .0055c (sealed)
16	c_l against gap	.02c	Varies
17	$\Delta ch_a\delta_a$ against Δc_l (showing change with M)	.02c	0.0055c
18	$\Delta ch_a\delta_a$ against Δc_l (showing effect of balance-nose radii) (by pressure distribution)	.02c	.0055c
19	$\Delta ch_a\delta_a$ against Δc_l (showing effect of gap)	.02c	Varies
20	$\Delta ch_a\delta_a$ against Δc_l (showing spread with α_o)	.02c	0.0055c

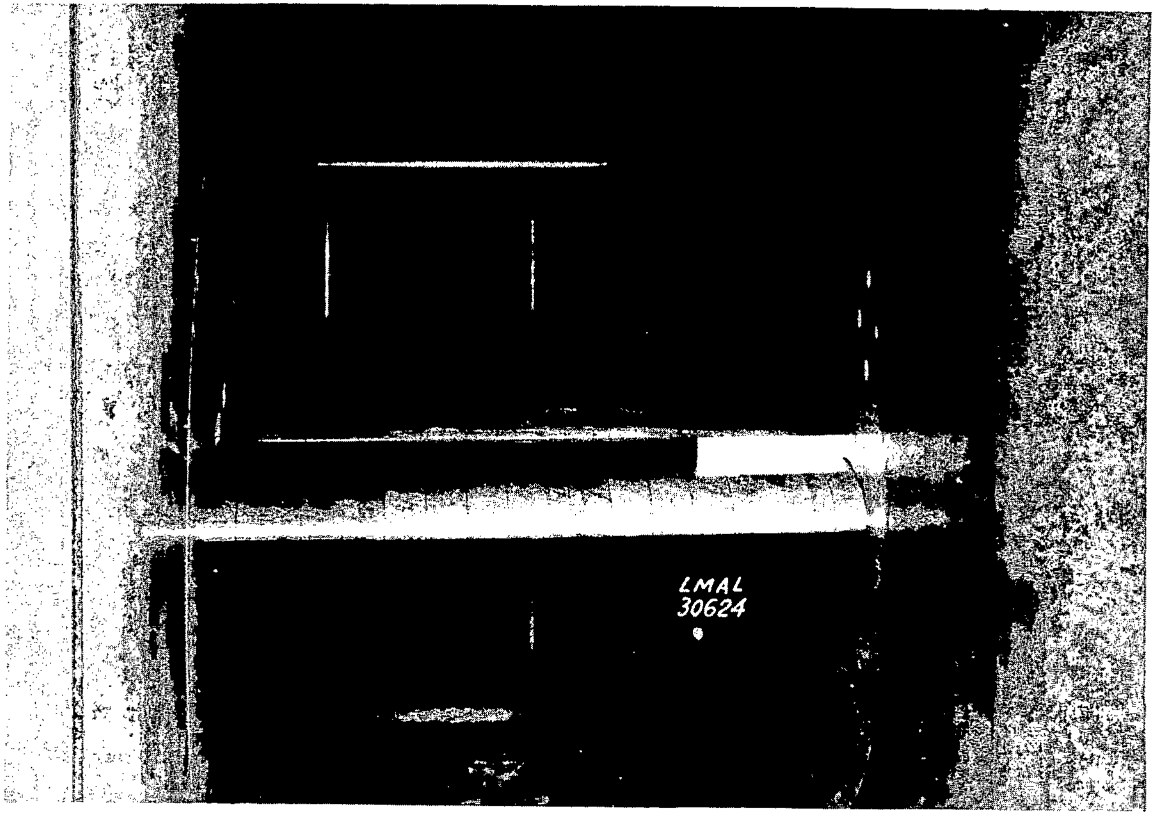

Figure 1.- Airfoil and aileron mounted in tunnel.

NACA

Fig. 2

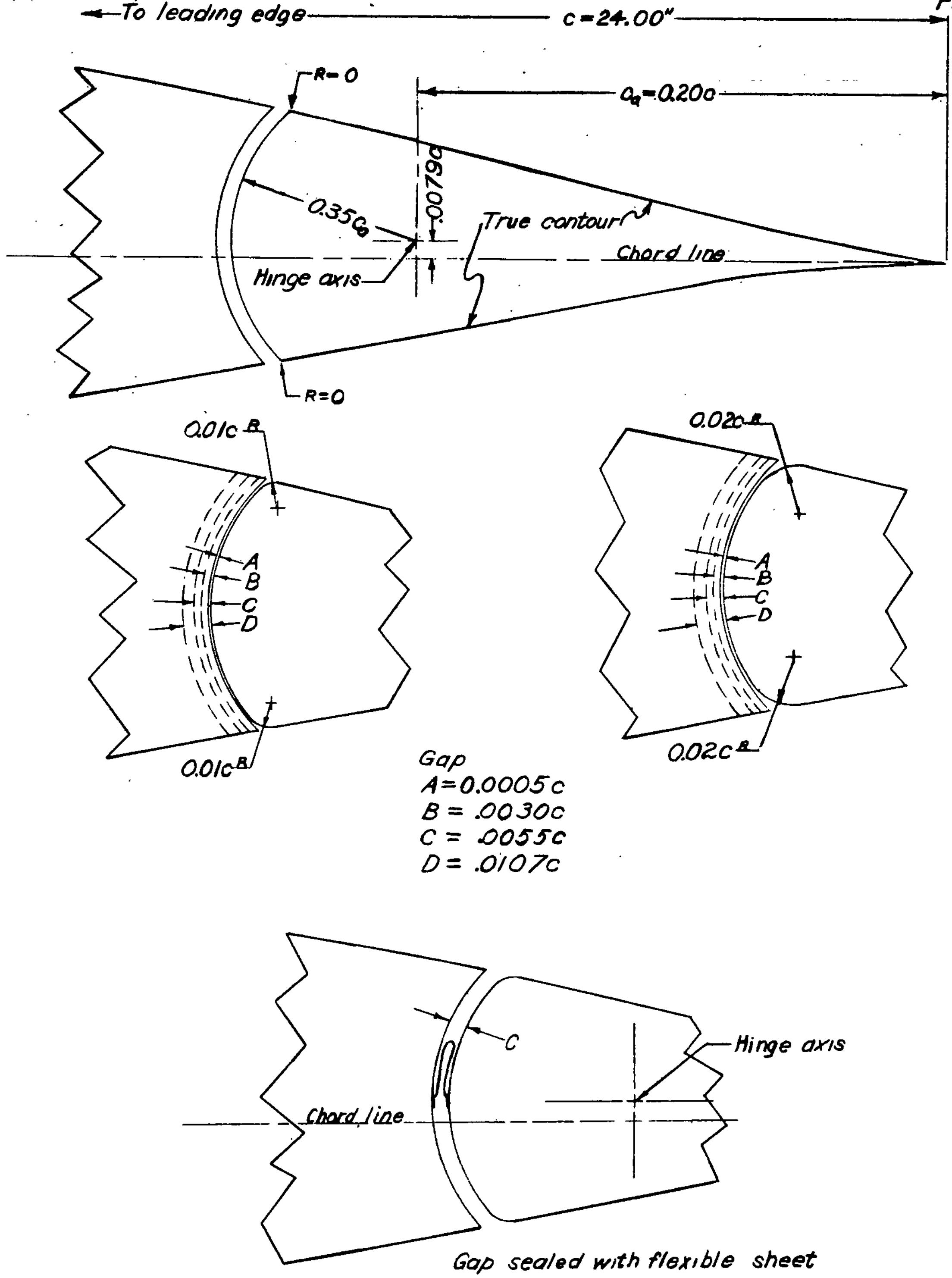

Figure 2.– Aileron section of NACA 66, 2-216, a=1.0 airfoil showing variations of balance-nose radii and gap.

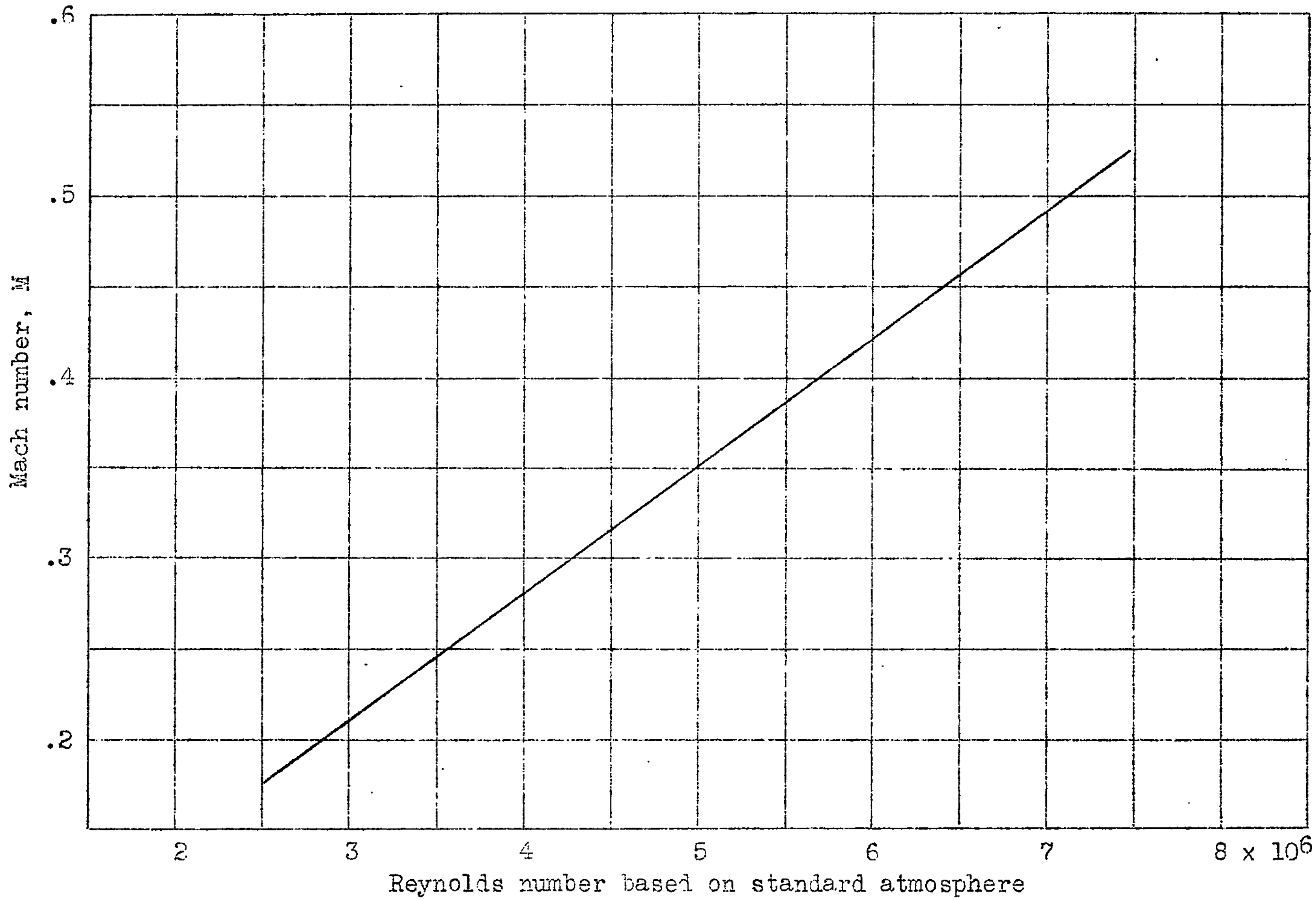

Figure 3.- Reynolds number for values of test Mach number for a 2-foot chord airfoil in the 2.5-by 6-foot test section of the stability tunnel.

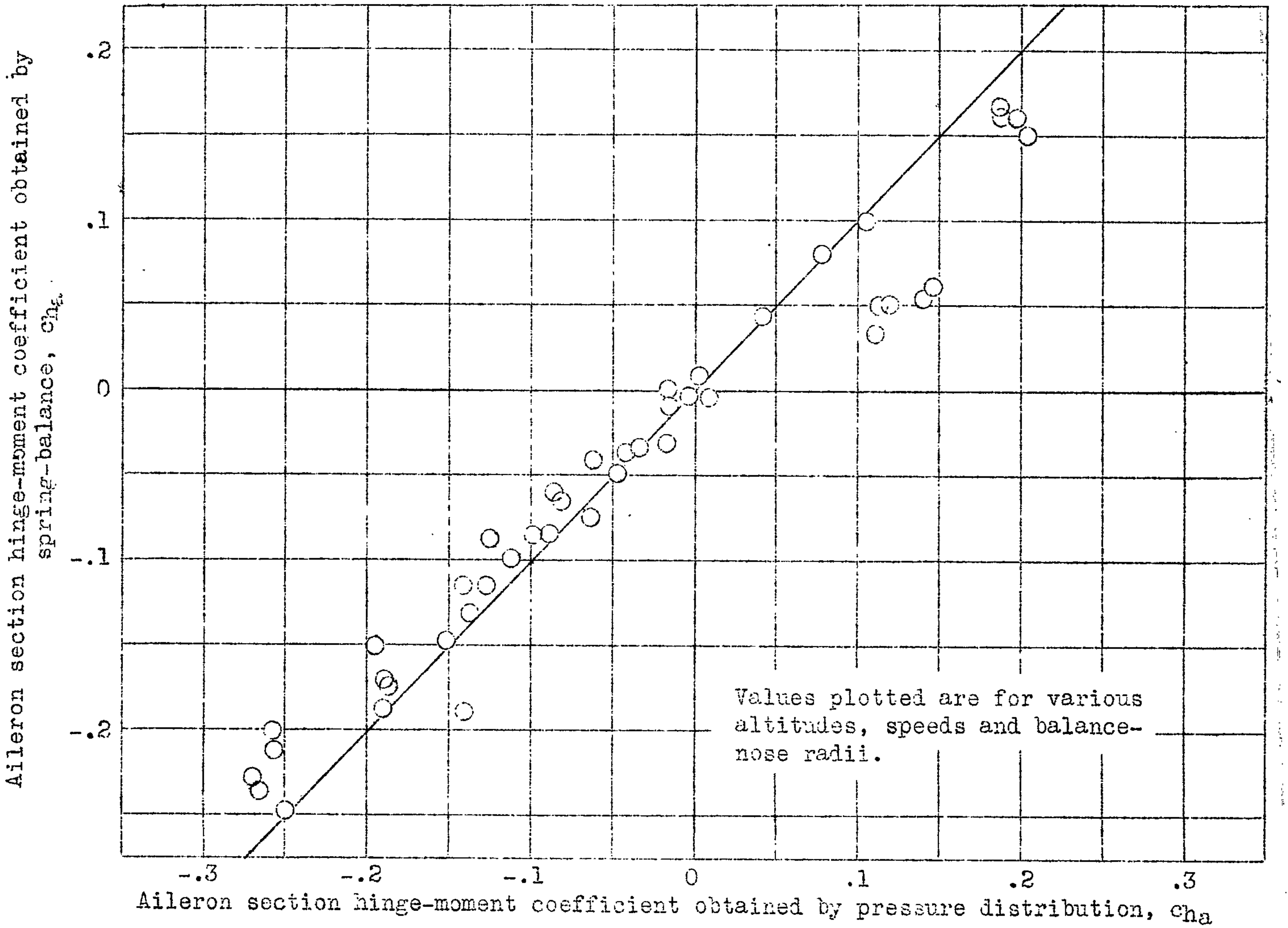

Figure 4.- A comparison between spring-balance and pressure-distribution section hinge-moment coefficients.

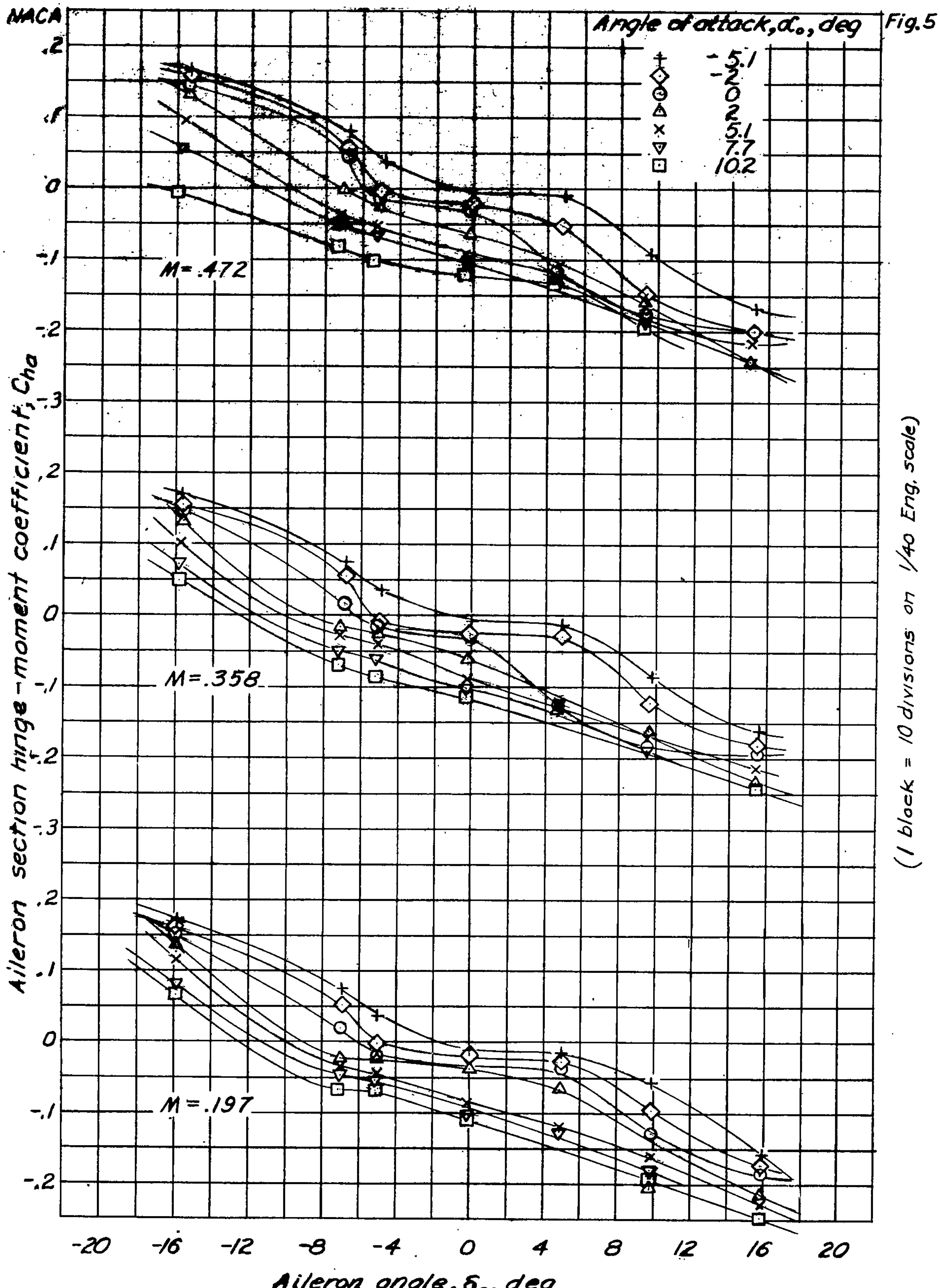

Figure 5.—Variation of aileron section hinge-moment coefficient with aileron angle (by pressure distribution). Balance-nose radii = 0; gap = 0.0055c.

L-431

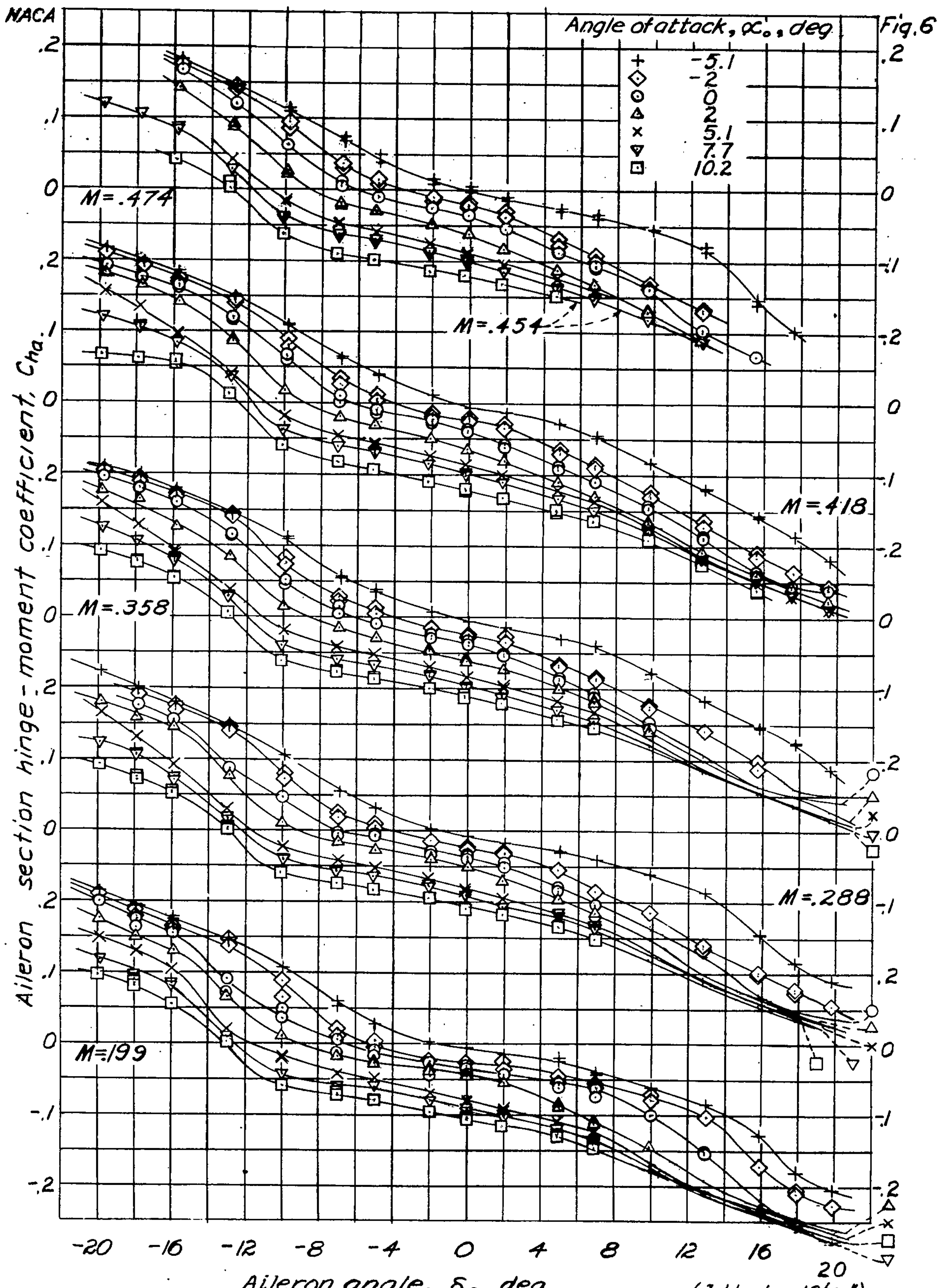

Figure 6.— Variation of aileron section hinge-moment coefficient with aileron aileron angle. Balance-nose radii = 0.01c; gap = 0.0055c.

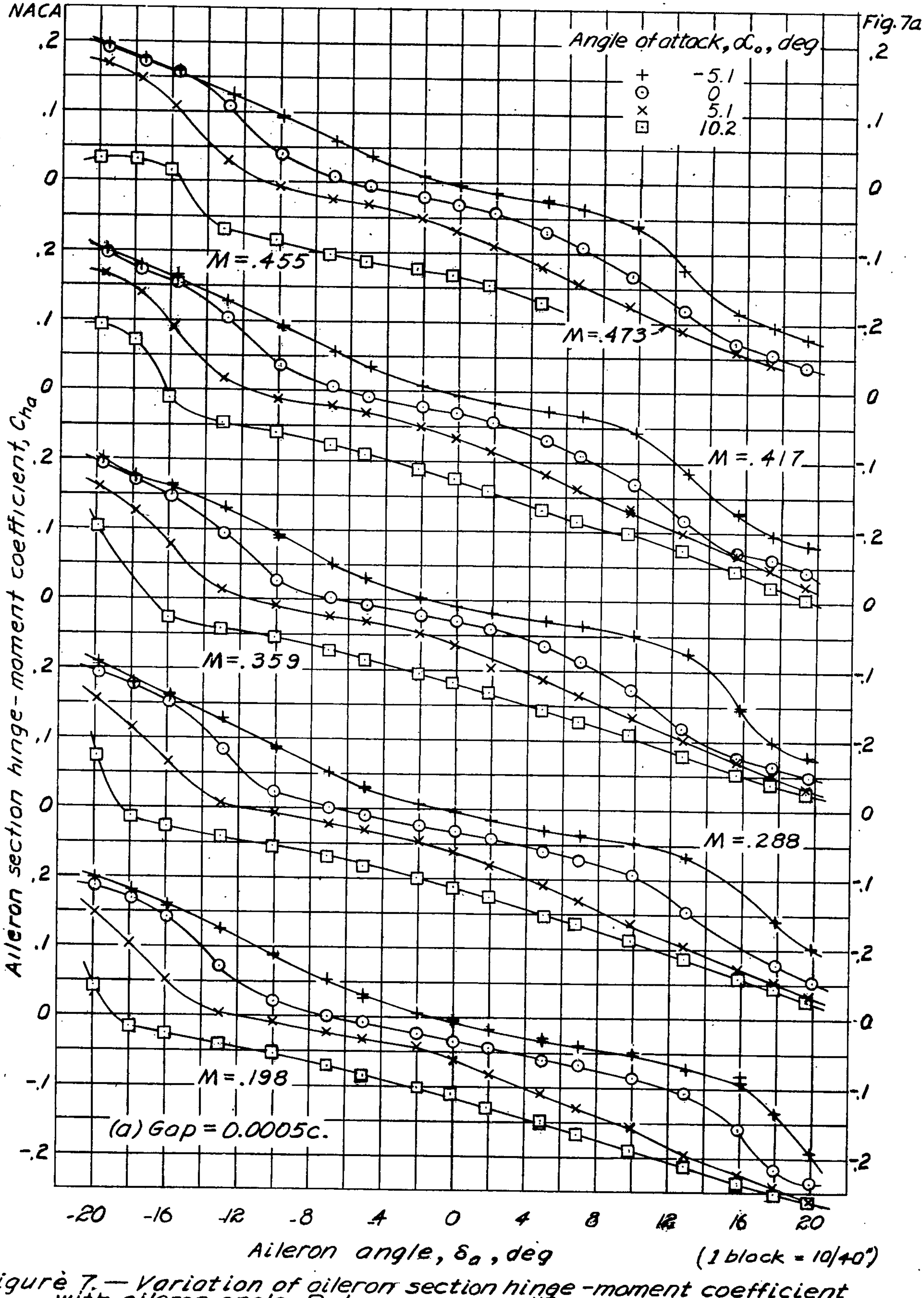

Figure 7.— Variation of aileron section hinge-moment coefficient with aileron angle. Balance-nose radii = 0.02c.

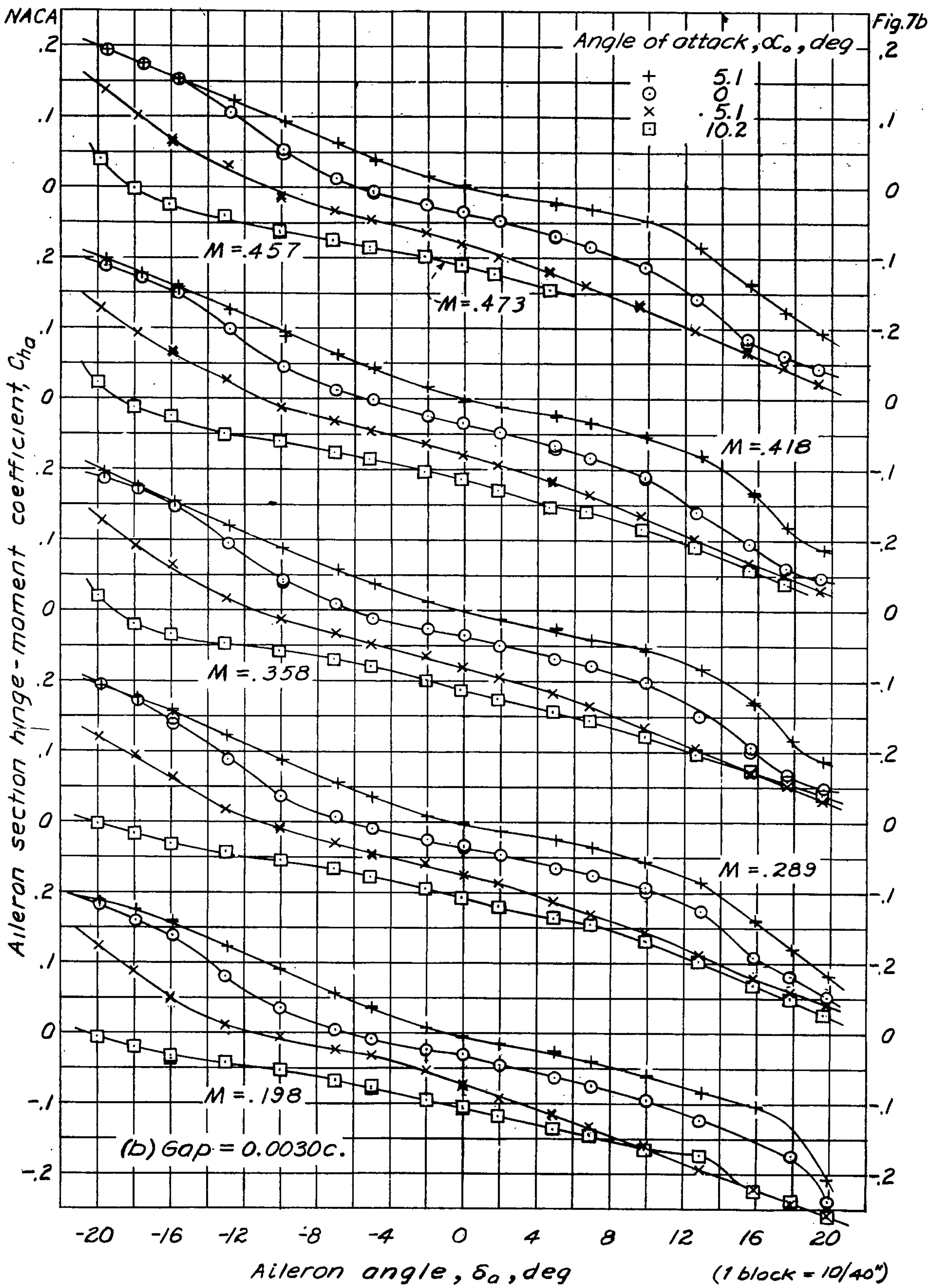

Figure 7. — Variation of aileron section hinge-moment coefficient with aileron angle. Balance-nose radii = 0.02c. (Continued)

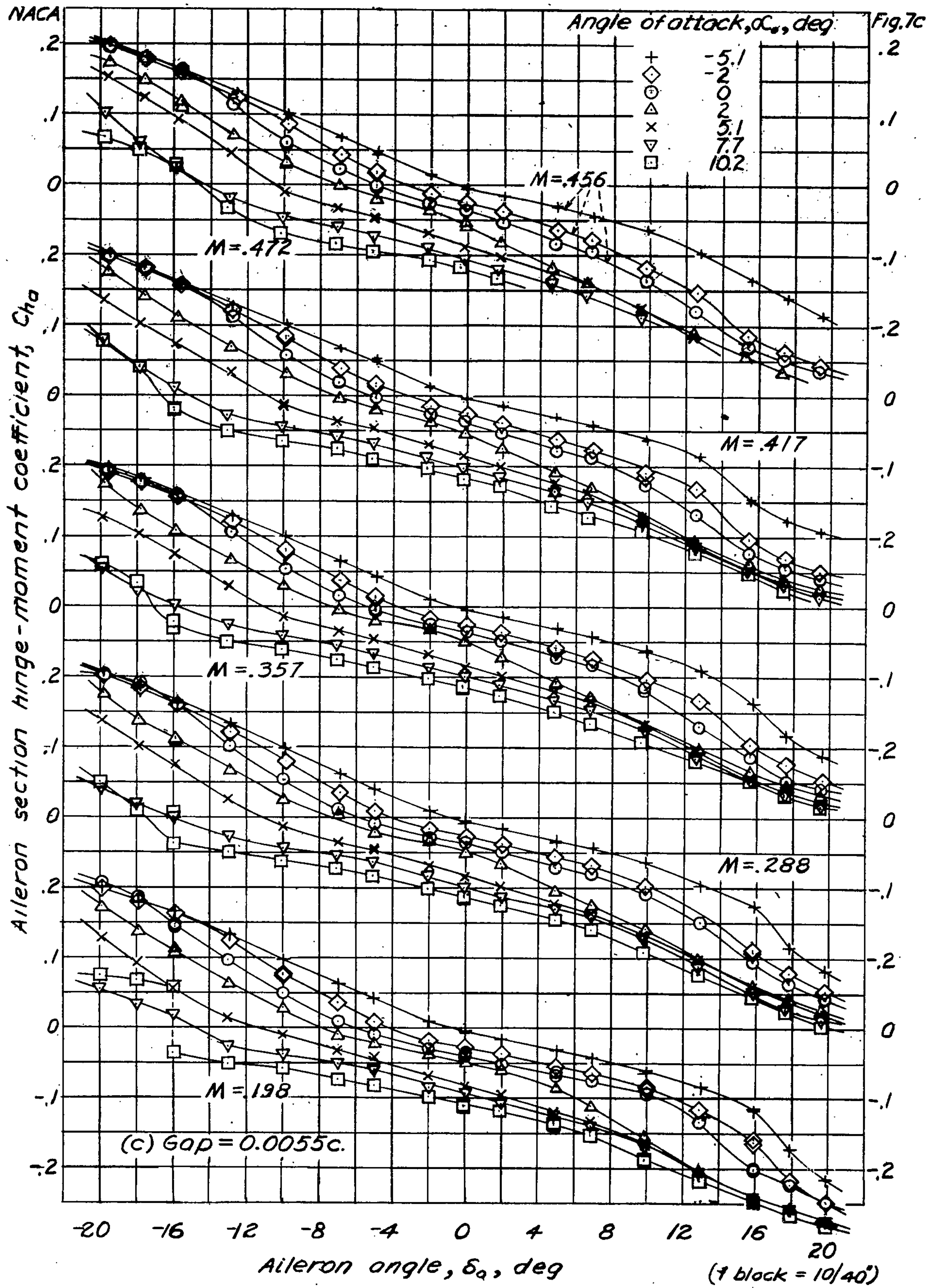

Figure 7.— Variation of aileron section hinge-moment coefficient with aileron angle. Balance-nose radii = 0.02c. (Continued)

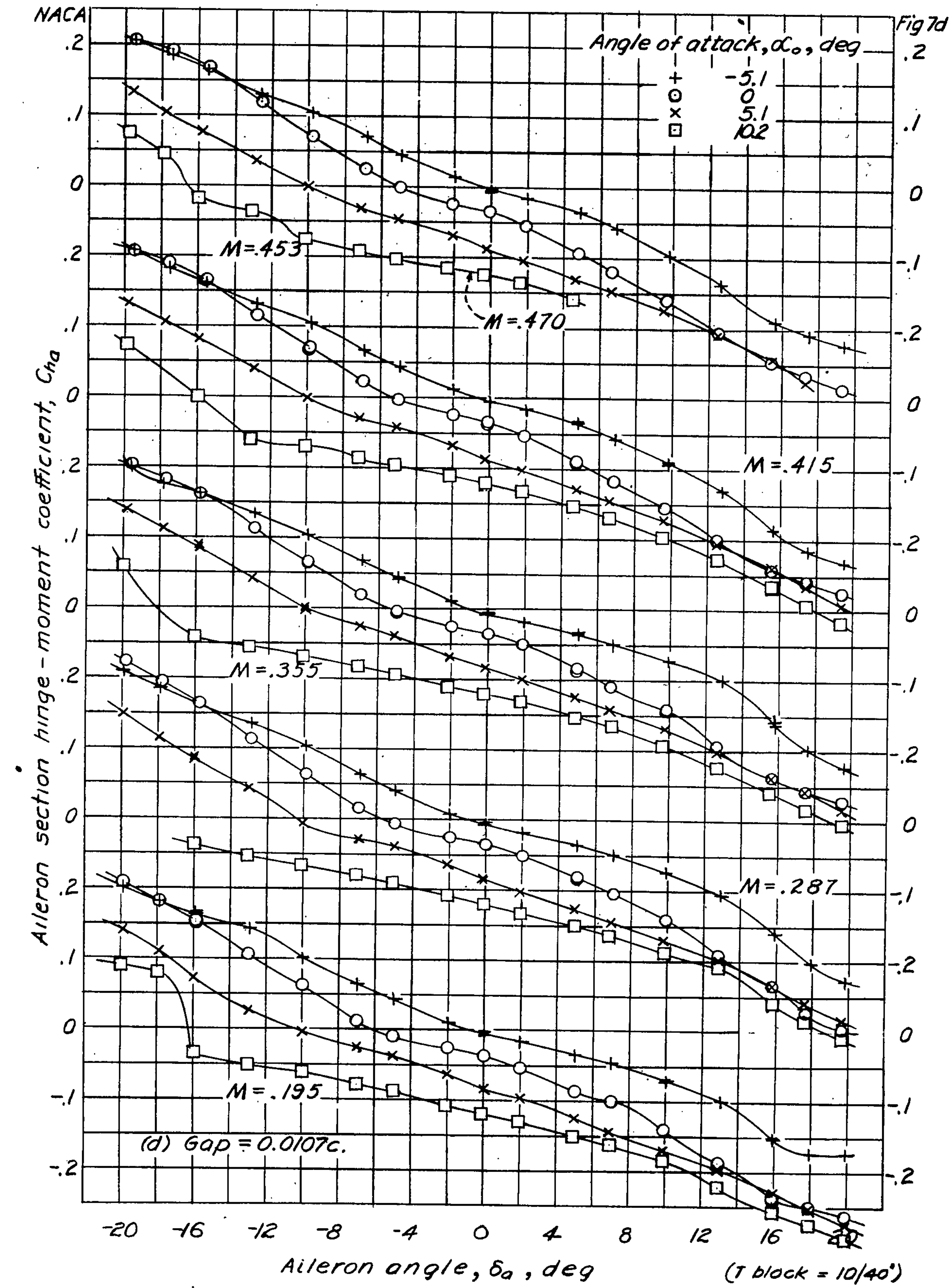

Figure 7.—Variation of aileron section hinge-moment coefficient with aileron angle. Balance-nose radii = 0.02c. (Continued)

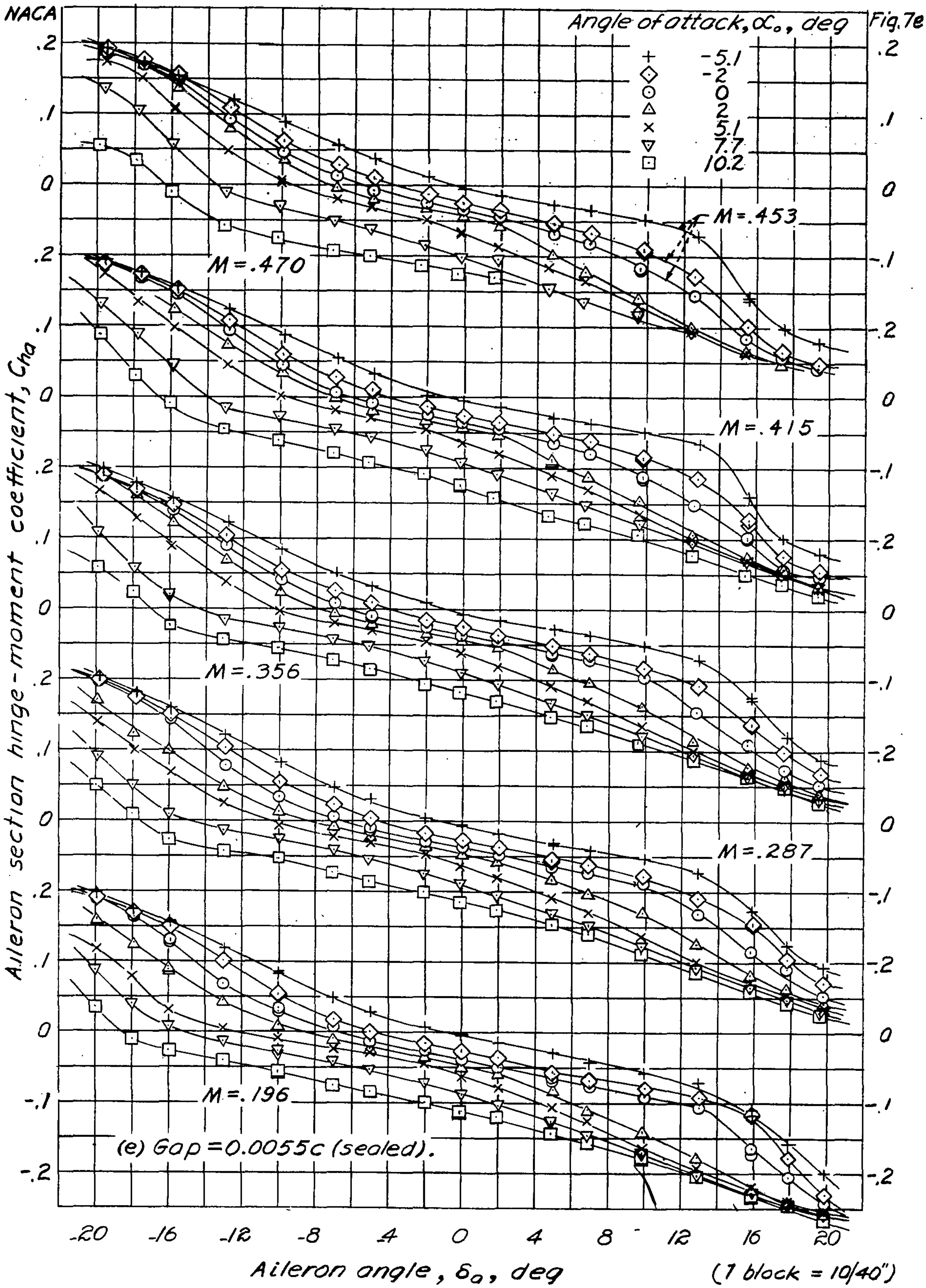

Figure 7.—Variation of aileron section hinge-moment coefficient with aileron angle. Balance-nose radii = 0.02c. (Concluded)

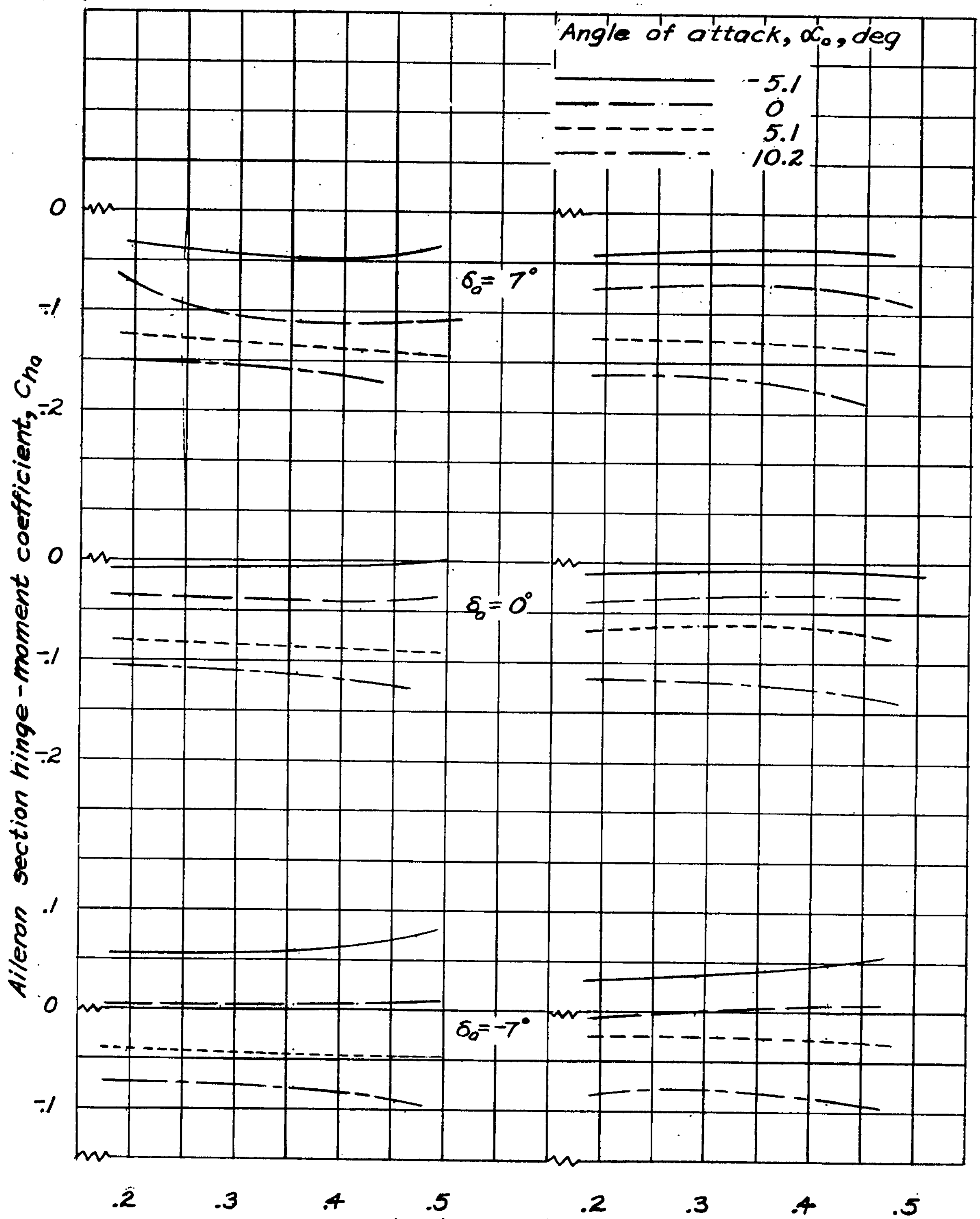

(a) Balance nose radii = 0.01c.

Gap = 0.0055c Gap = 0.0055c (sealed)

Figure 8. — Variation of aileron section hinge-moment coefficient with Mach number.

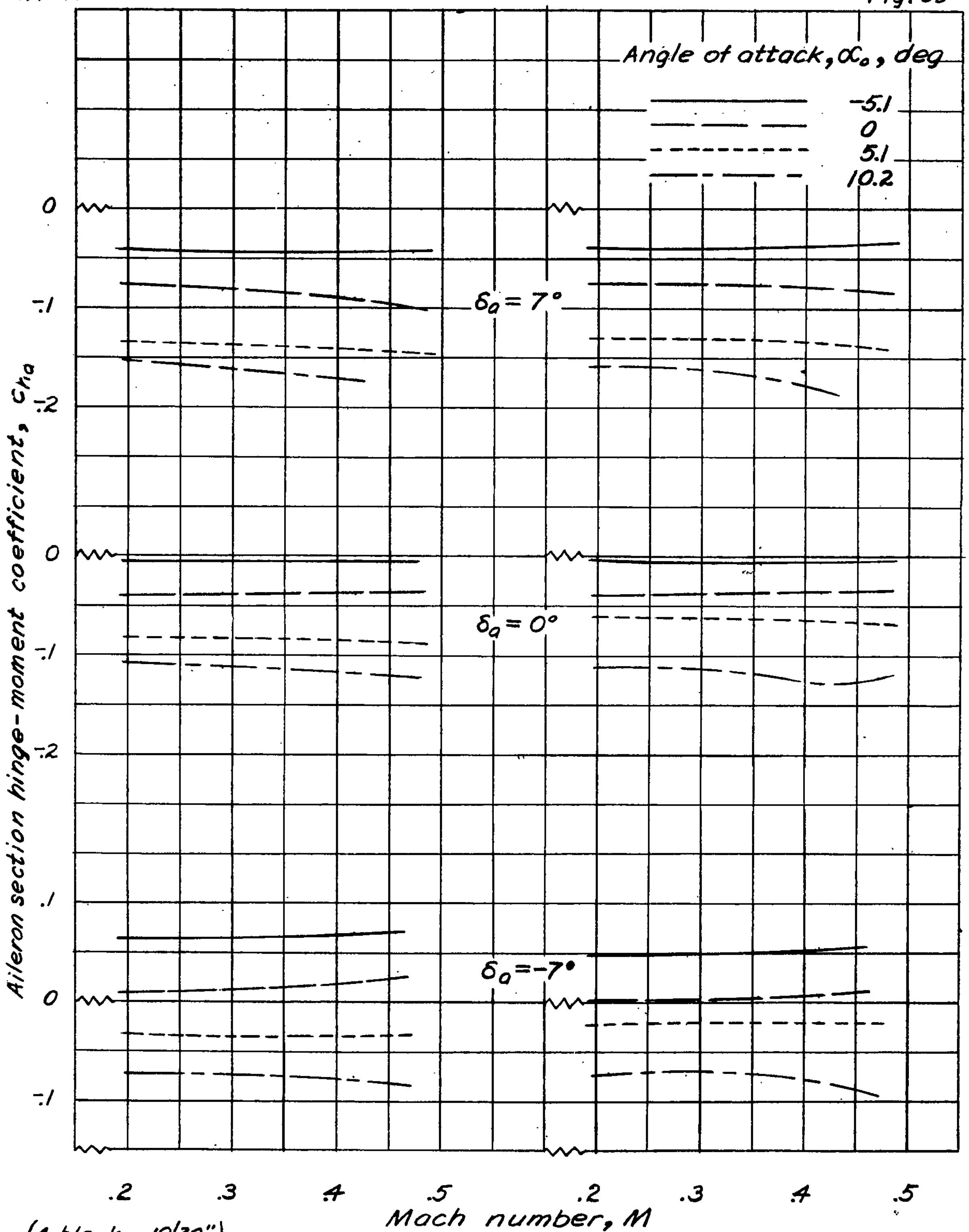

(b) Balance nose radii = 0.02c.
Gap = 0.0055 c Gap = 0.0055 c (sealed)

Figure 8.— Variation of aileron section hinge-moment coefficient with Mach number. (Concluded)

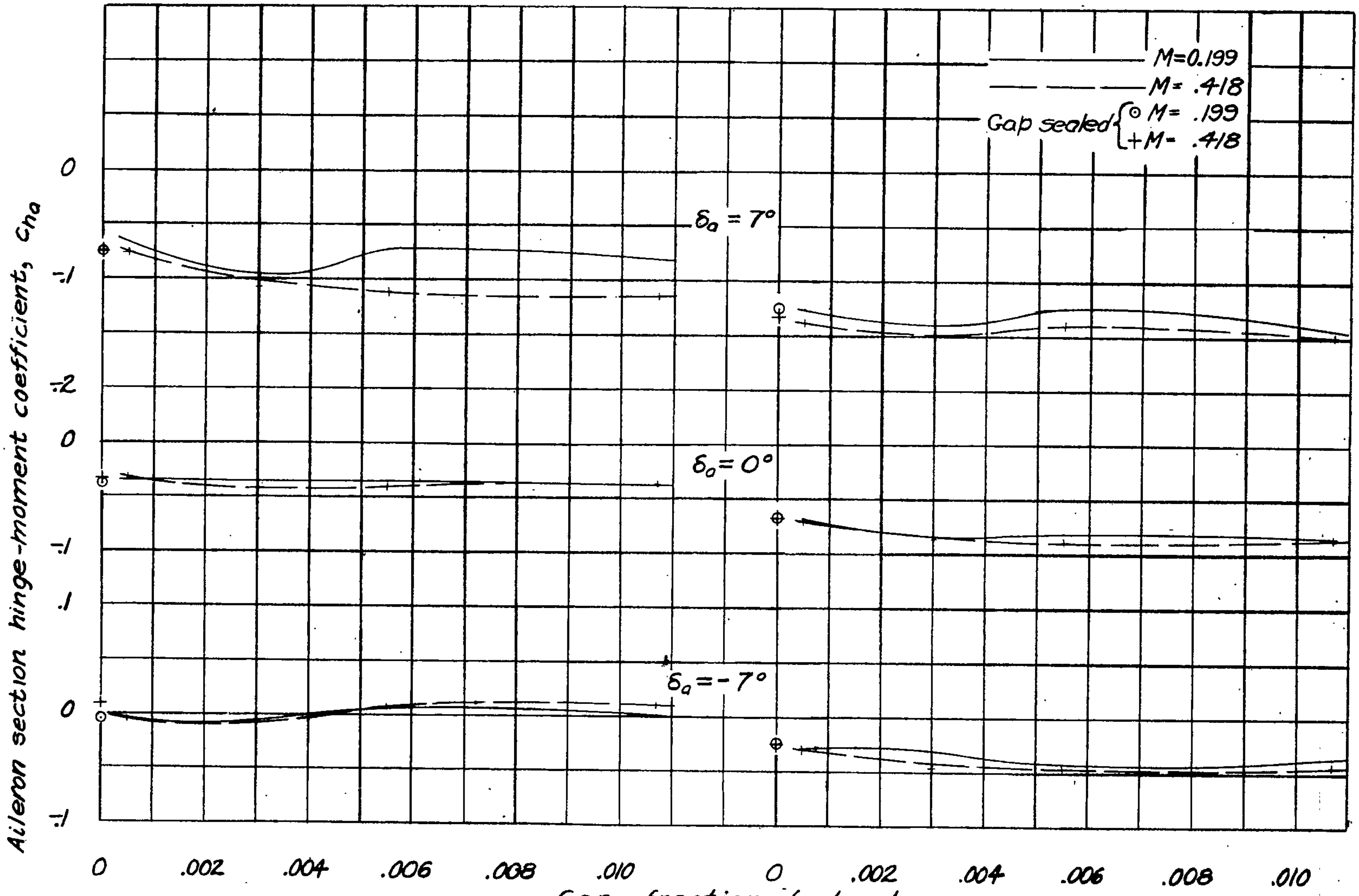

(a) Balance-nose radii = 0.01c.

$\alpha_0 = 0°$ $\alpha_0 = 5.1°$

(1 block = 10/30")

Figure 9.— Variation of aileron section hinge-moment coefficient with gap.

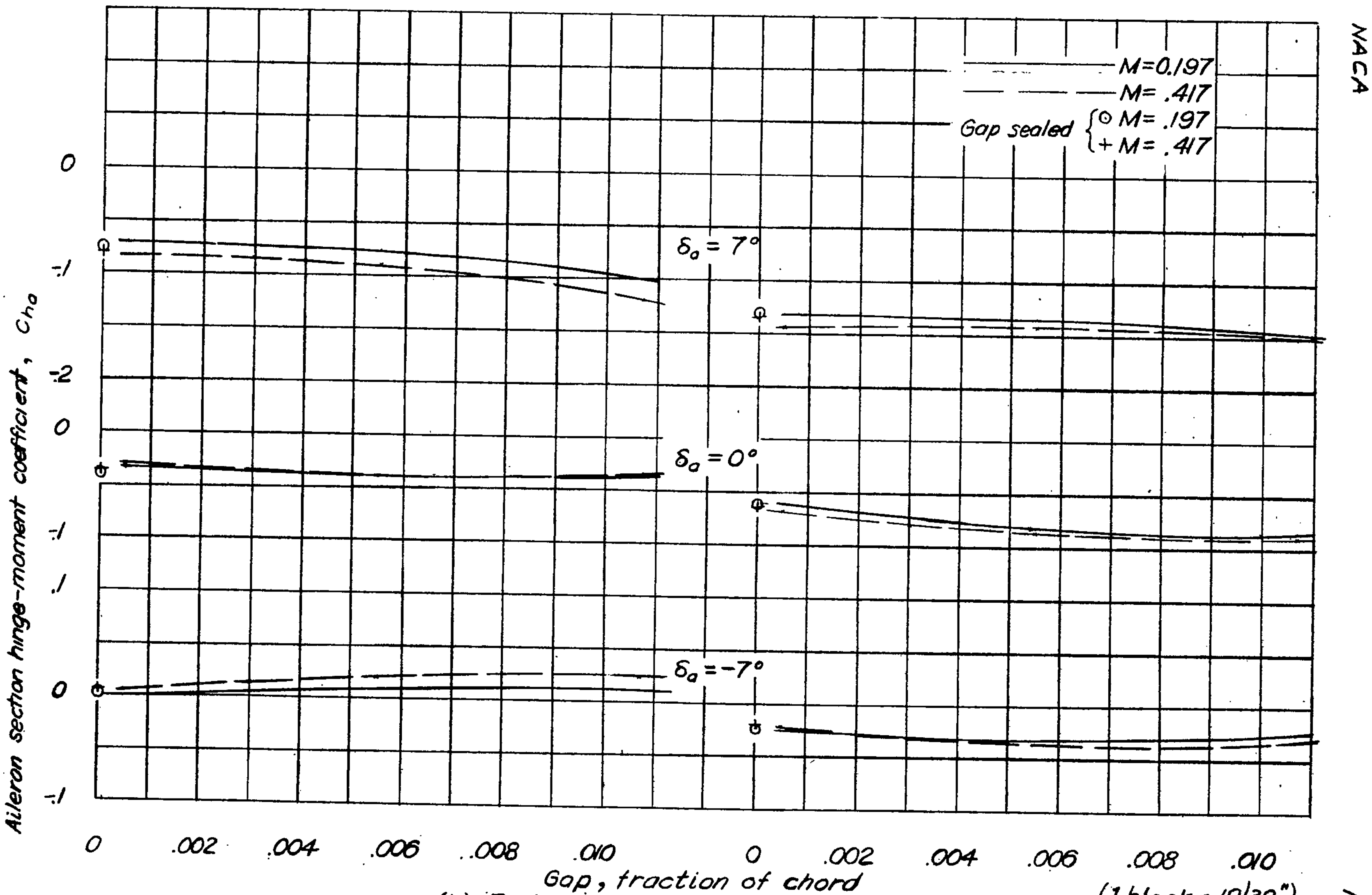

(b) Balance-nose radii = 0.02c.

Figure 9.– Variation of aileron section hinge-moment coefficient with gap. (Continued)

Fig. 9b

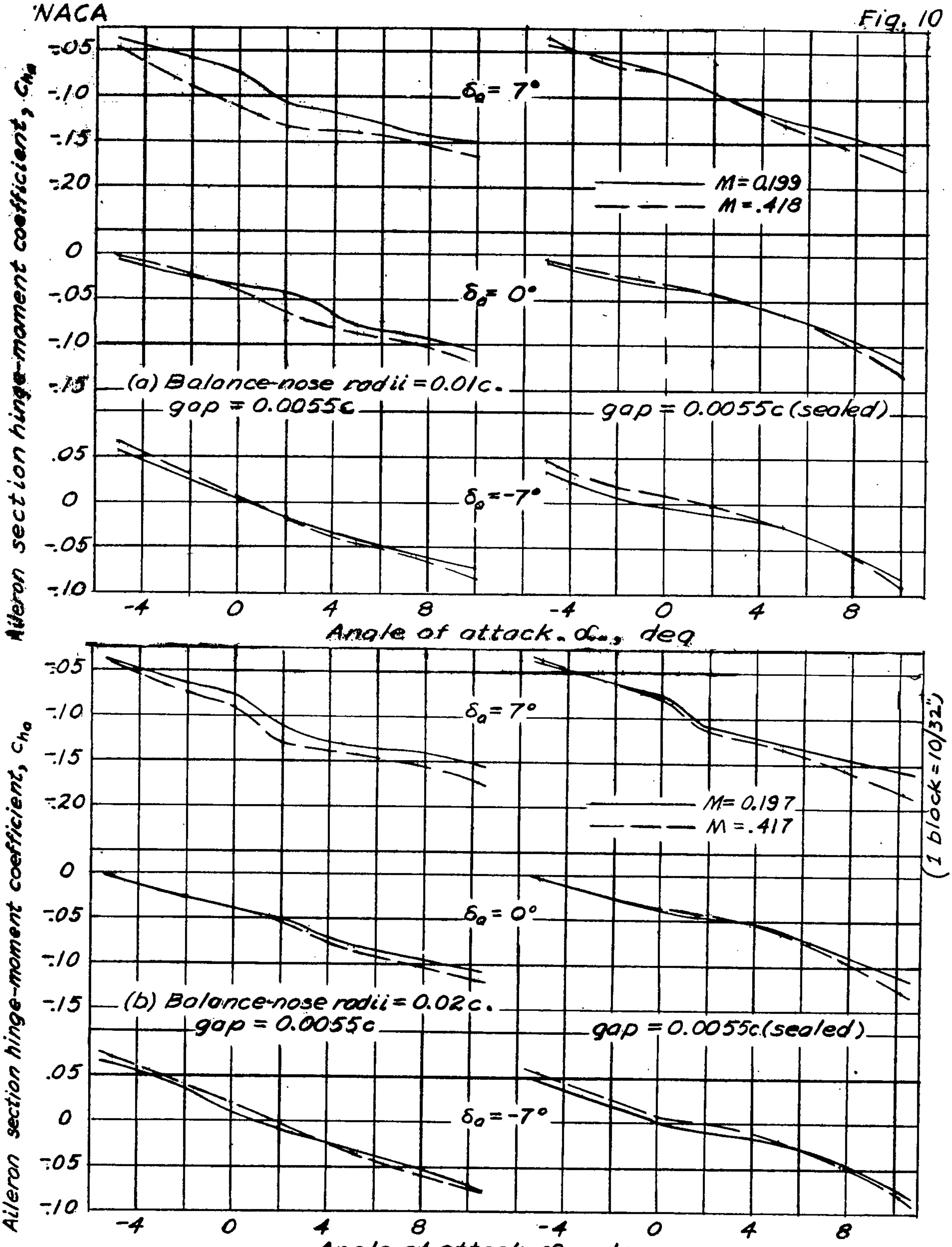

Figure 10.— Variation of aileron section hinge-moment coefficient with angle of attack.

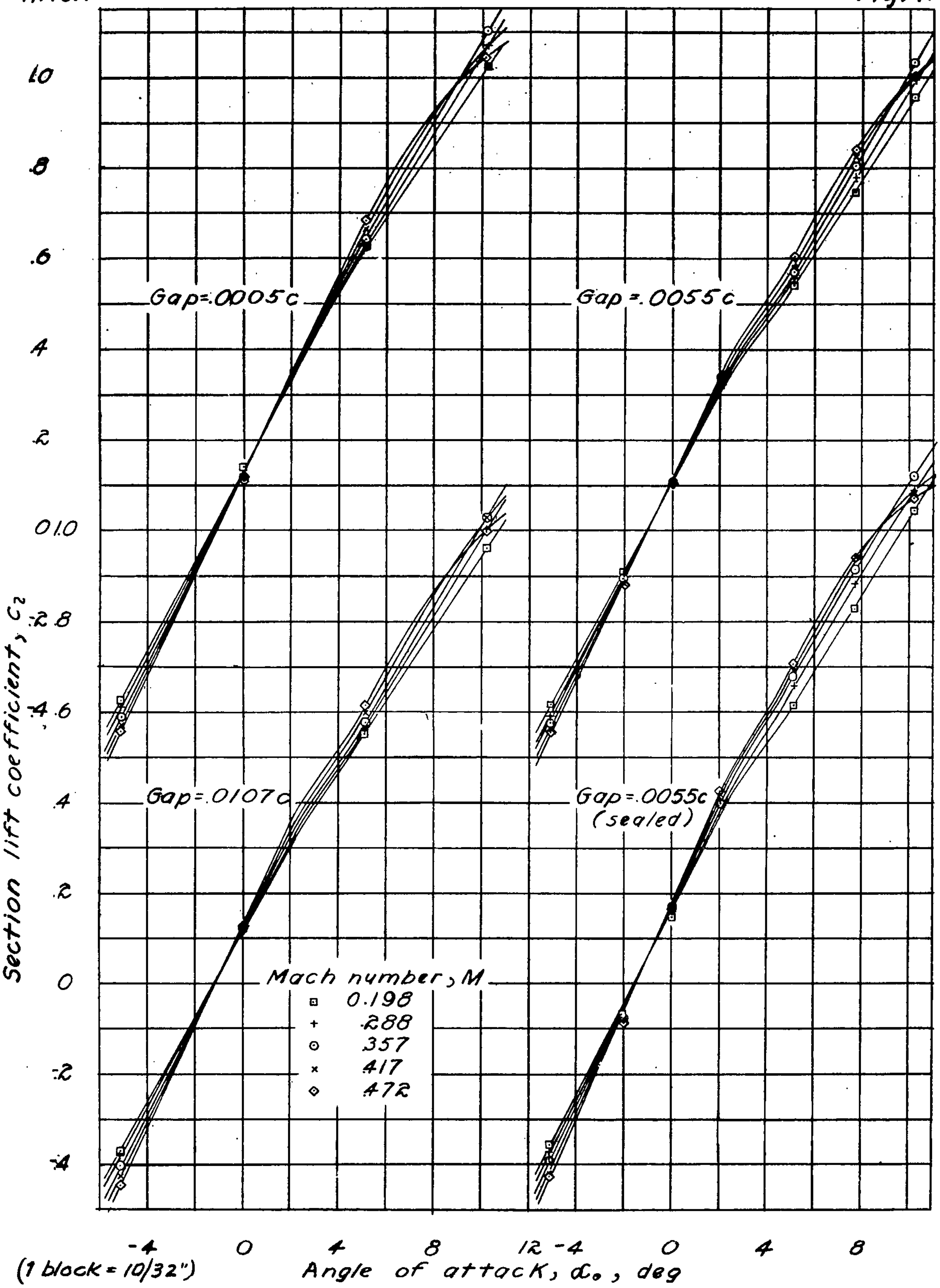

Figure 11.— Variation of section lift coefficient with angle of attack. Balance-nose radii = 0.02c; $\delta_a = 0°$.

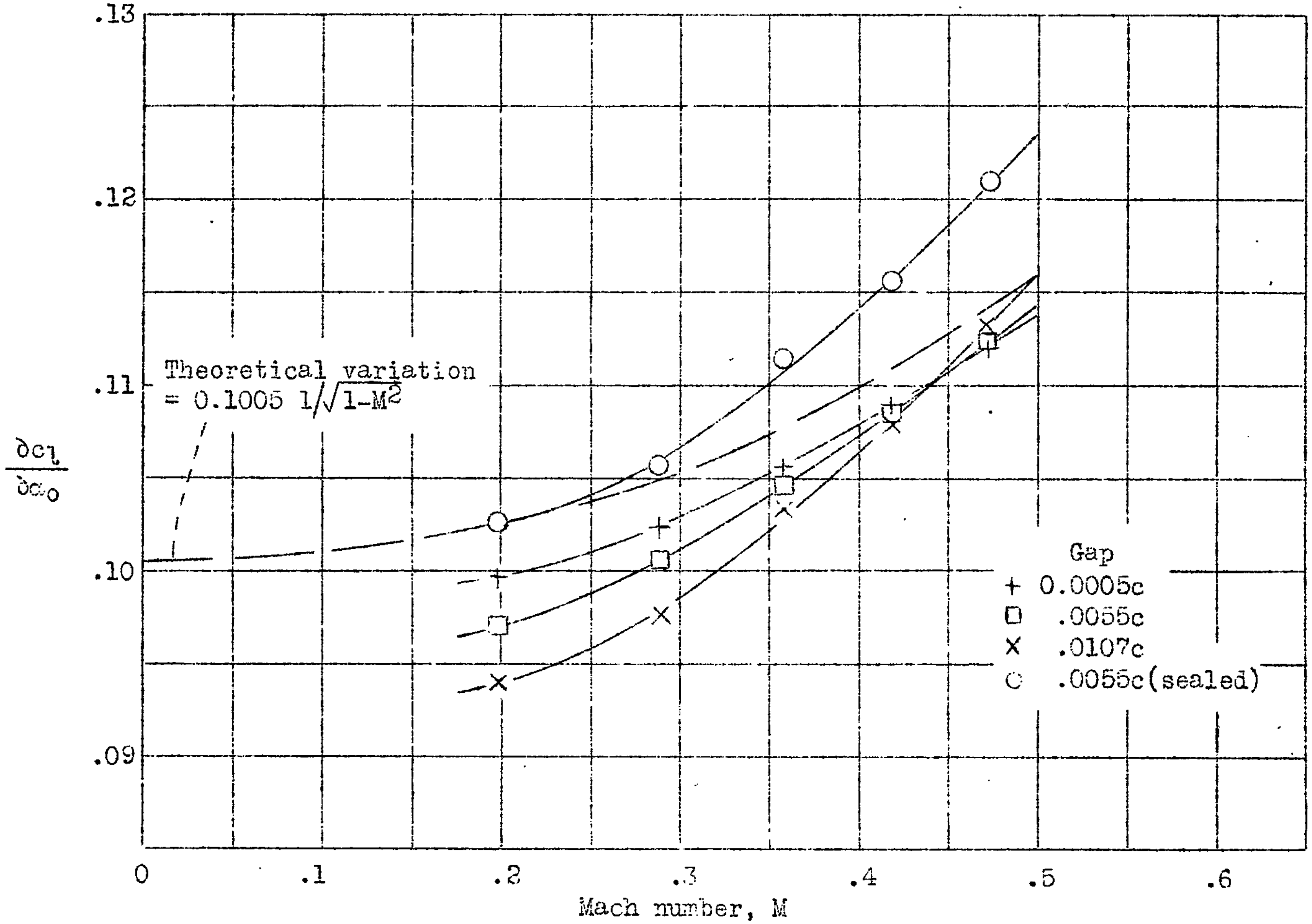

Figure 12.- Variation of lift curve slope $\partial c_l/\partial \alpha$ with Mach number for various gap widths. $\delta_a = 0$.

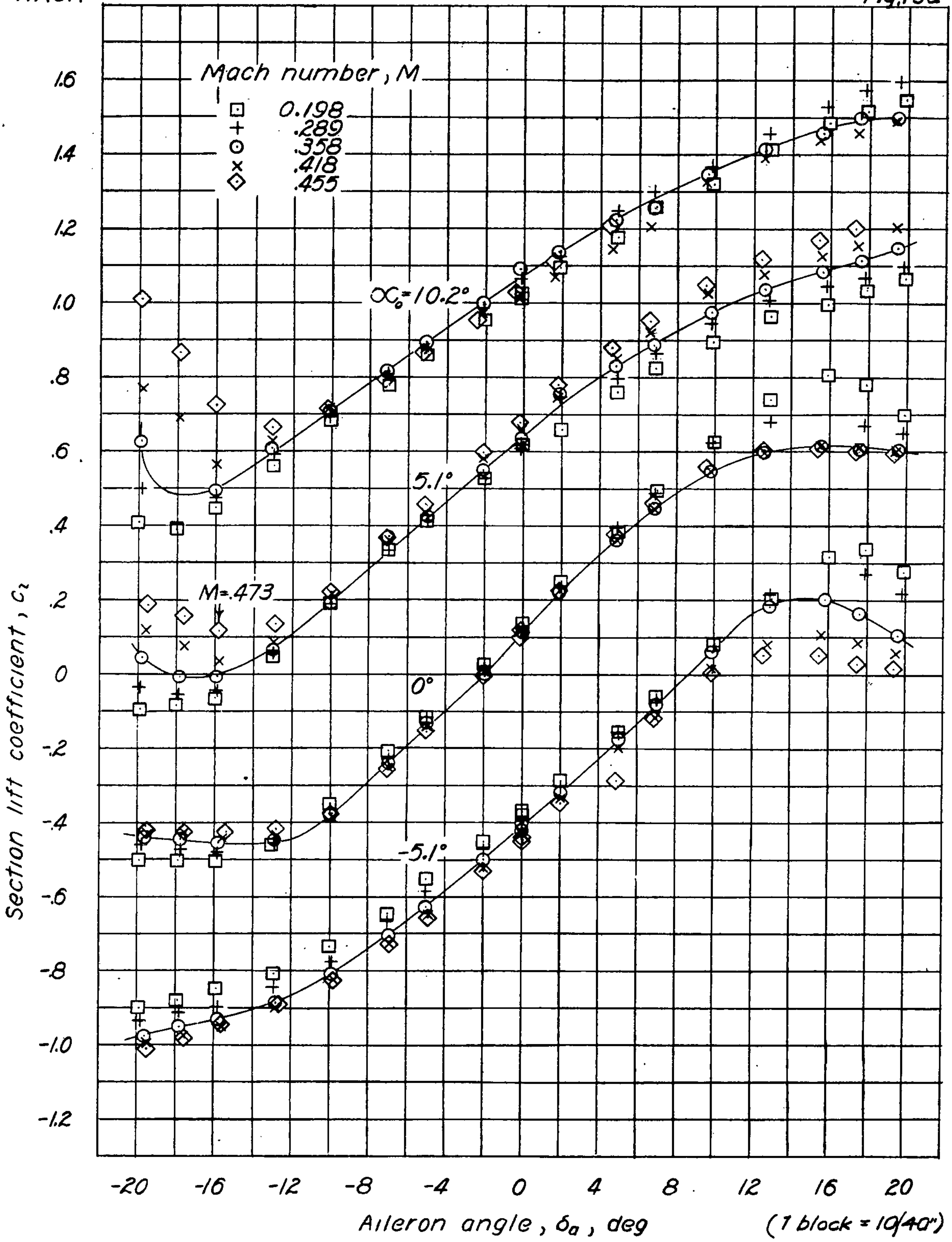

(a) Gap = 0.0005c.

Figure 13.— Variation of section lift coefficient with aileron angle. Balance-nose radii = 0.02c.

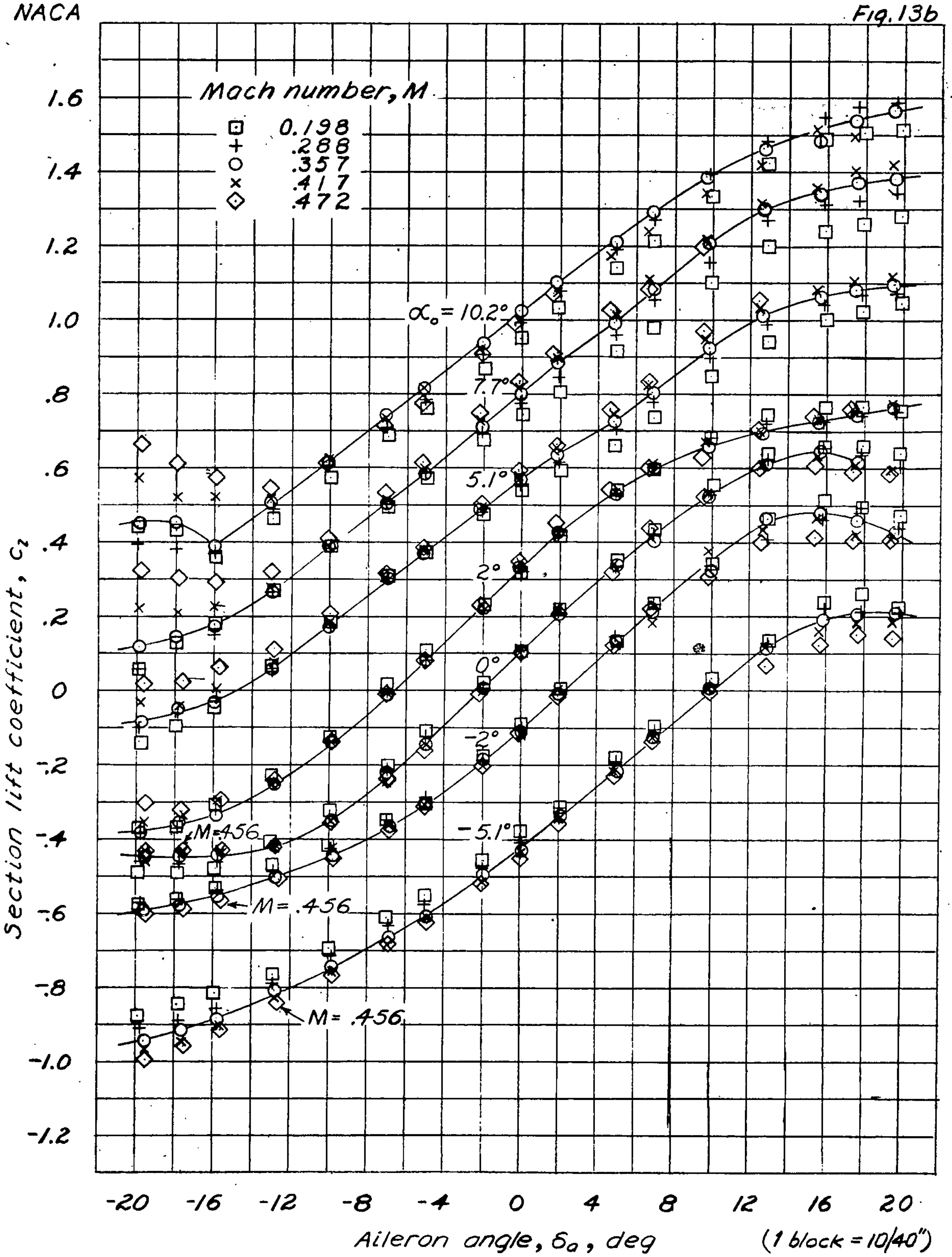

(b) Gap = 0.0055c.

Figure 13. — Variation of section lift coefficient with aileron angle. Balance-nose radii = 0.02c. (Continued)

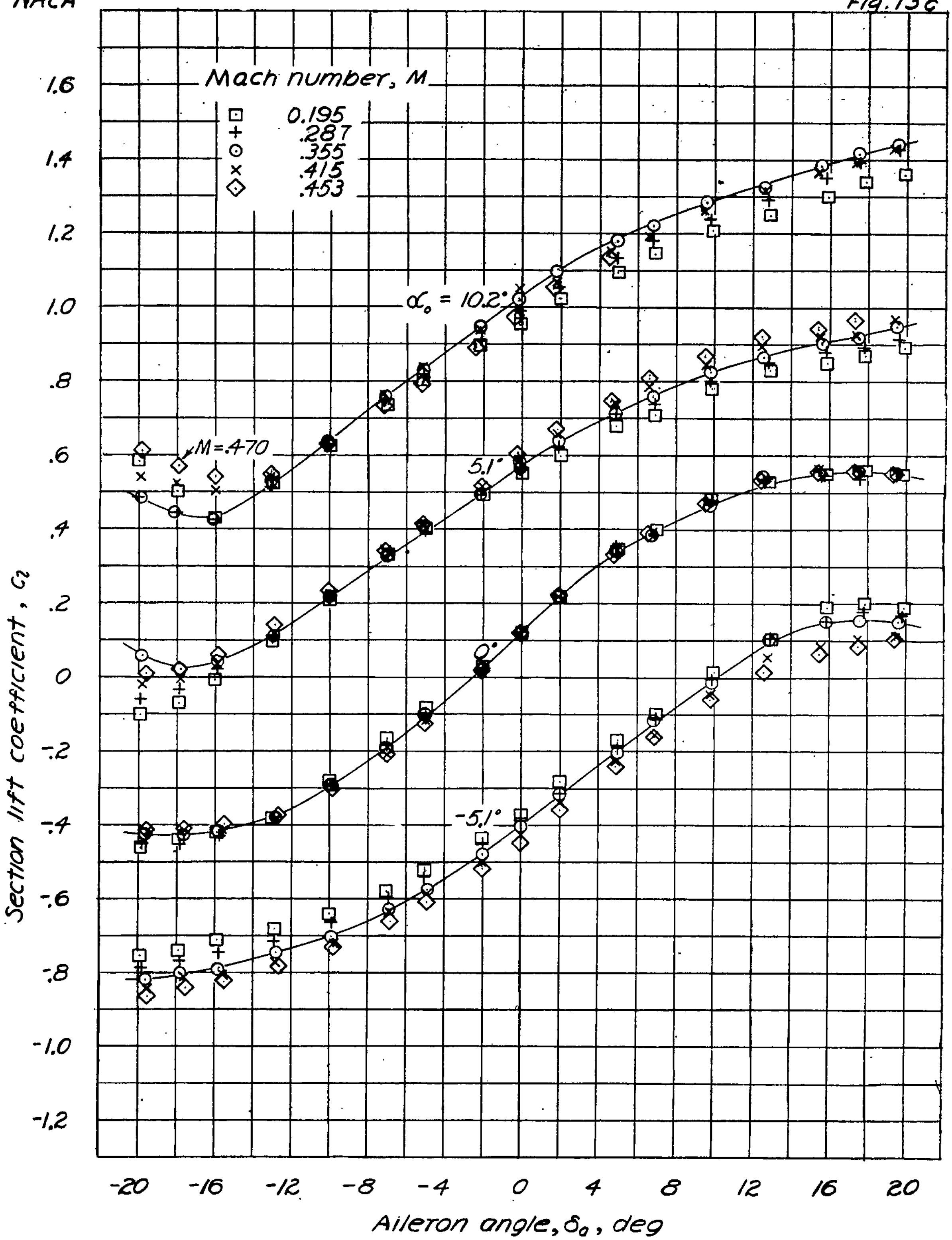

(c) Gap = 0.0107c. (1 block = 10/40")

Figure 13. – Variation of section lift coefficient with aileron angle Balance-nose radii = 0.02c. (Continued)

L-431

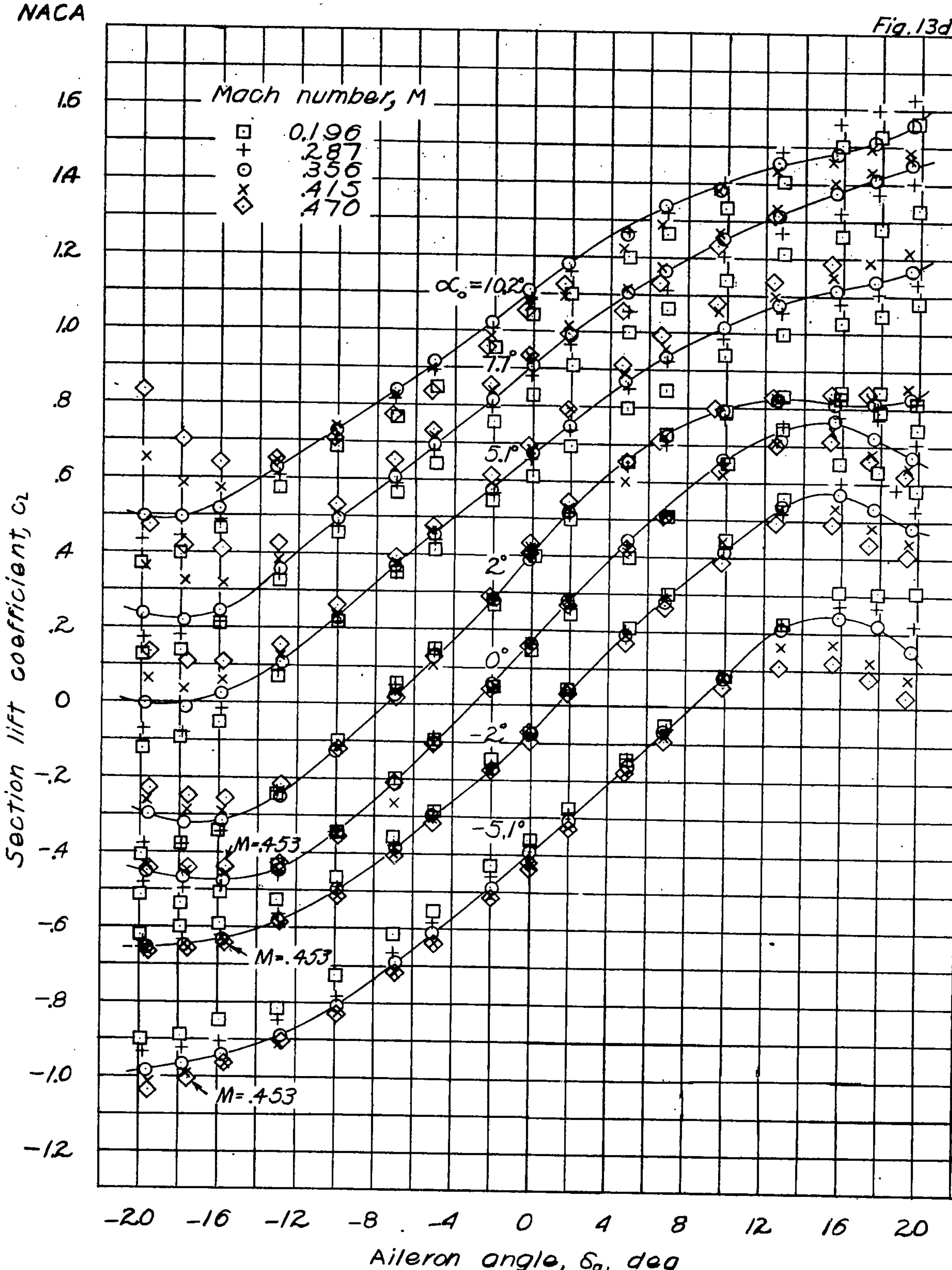

(d) Gap = 0.0055c sealed.

Figure 13. — Variation of section lift coefficient with aileron angle Balance nose radii = 0.02c. (Concluded)

L-431

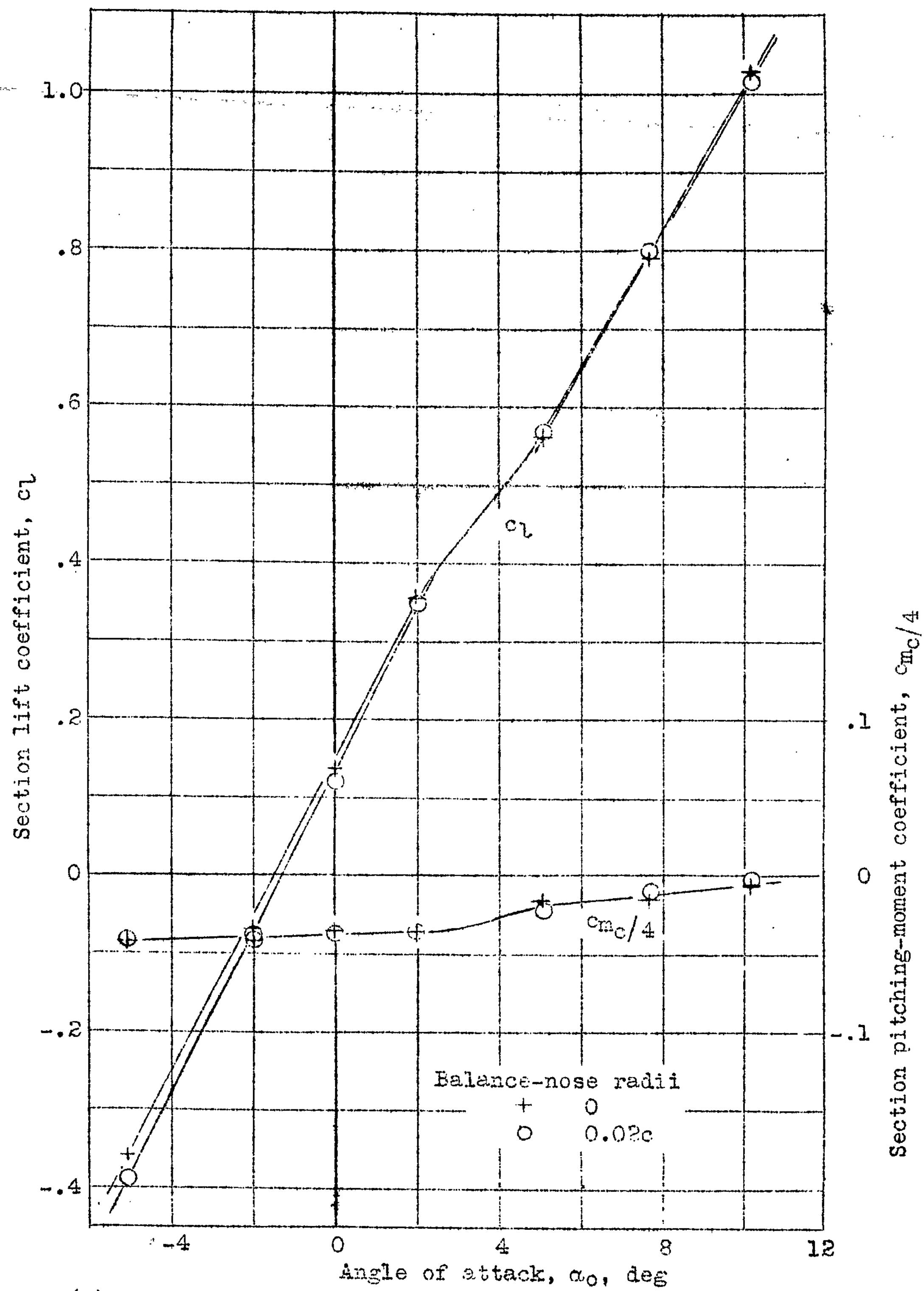

(a) Variation with α_o; $\delta_a = 0^\circ$.

Figure 14(a,b).- Section lift coefficients and section pitching-moment coefficients obtained by pressure-distribution. M = 0.358; gap = 0.0055c.

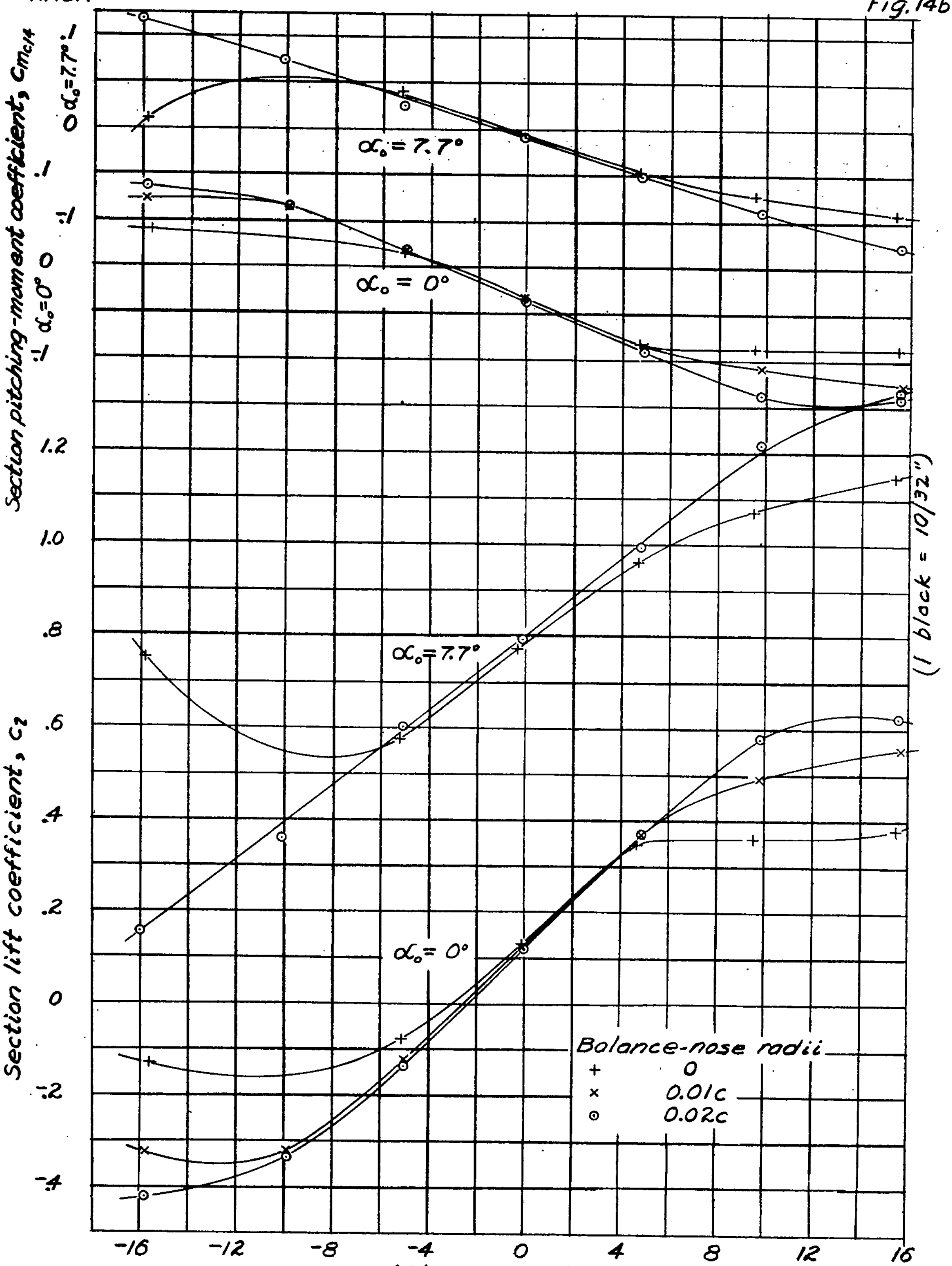

(b) Variation with δ_a.

Figure 14.— Section lift coefficients and section pitching-moment coefficients obtained by pressure-distribution. $M=0.358$; gap $=0.0055c$. (Concluded).

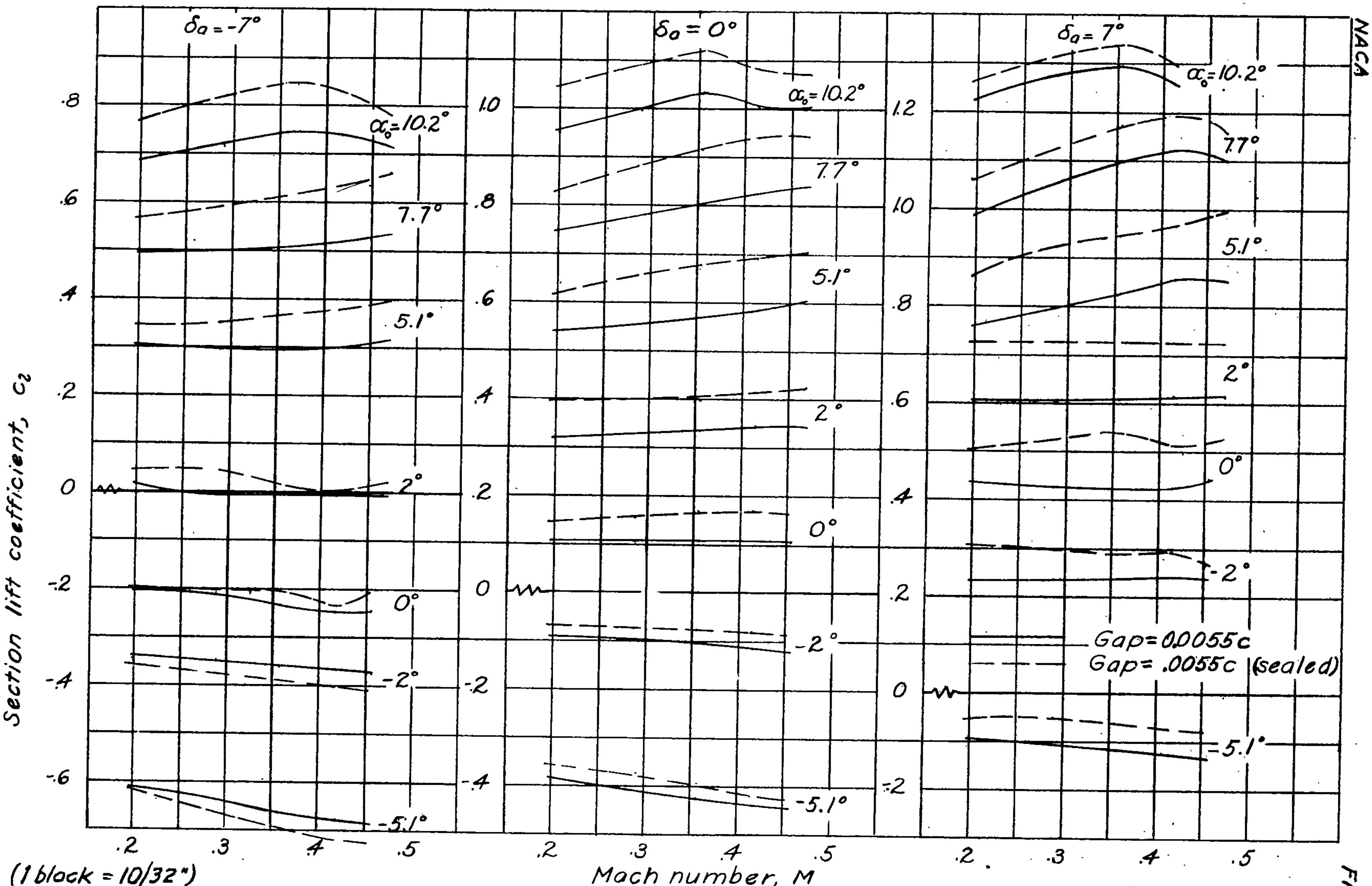

Figure 15.— Variation of section lift coefficient with Mach number
Balance-nose radii = 0.02 c.

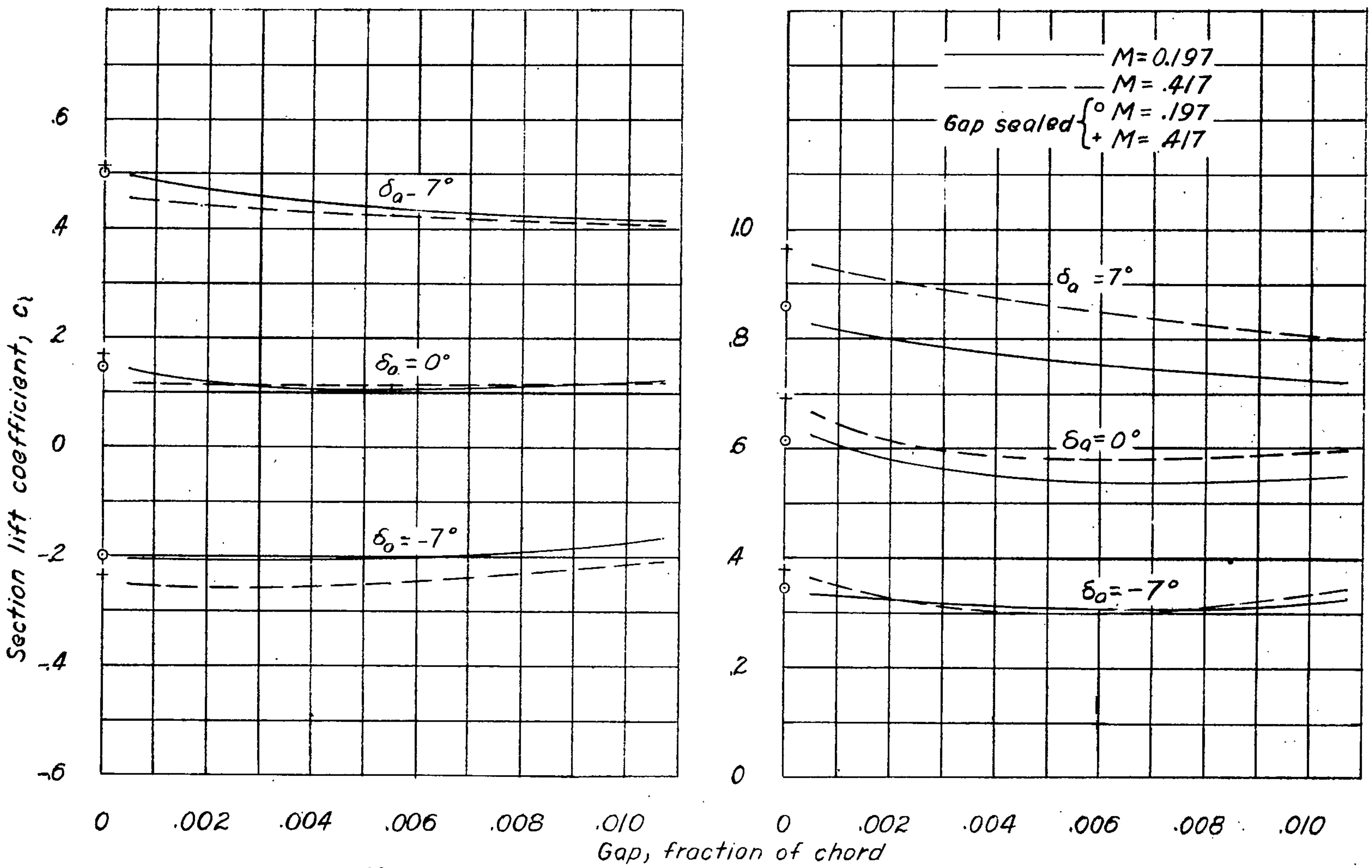

Figure 16.- Variation of section lift coefficient with gap.
Balance nose radii = 0.02c.

(1 block = 10/30")

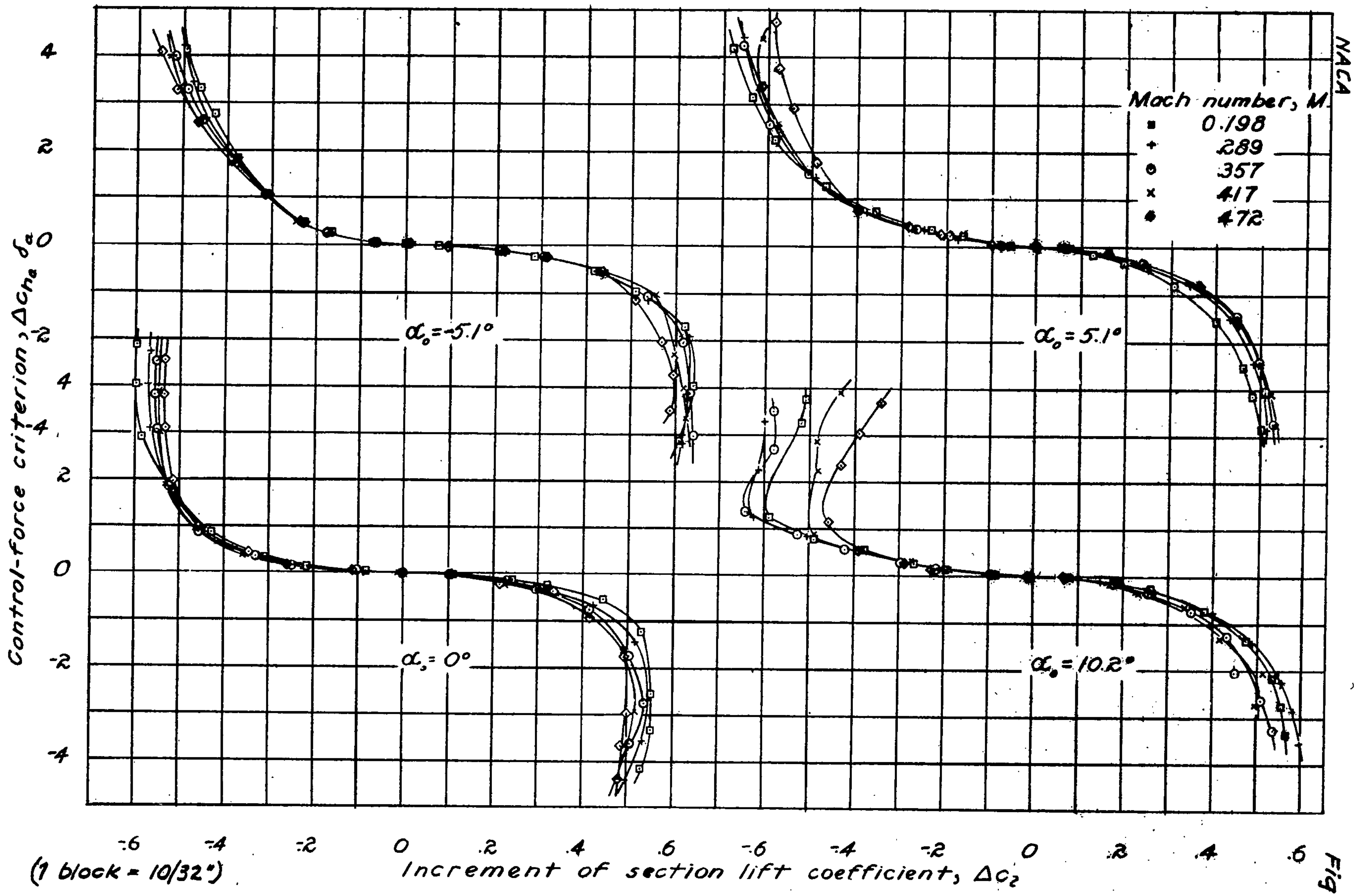

Figure 17. - Variation of control-force criterion with increment of section lift coefficient; showing change with Mach number. Balance nose radii = 0.02c; gap = 0.0055c.

L-431

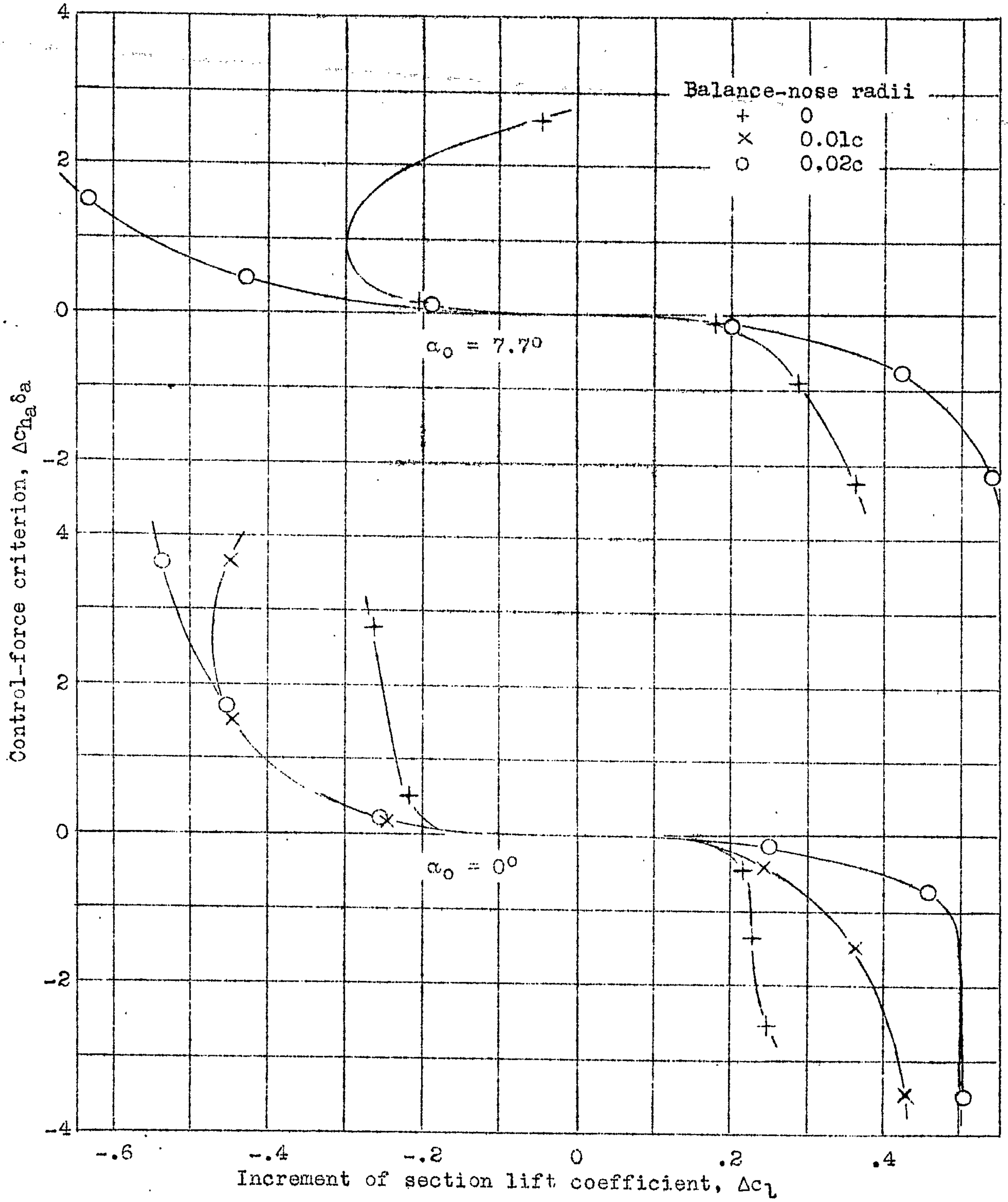

Figure 18.- Variation of $\Delta c_{h_a}\delta_a$ with Δc_l (by pressure distribution) showing effect of balance-nose radii. M = 0.358; gap = 0.0055c.

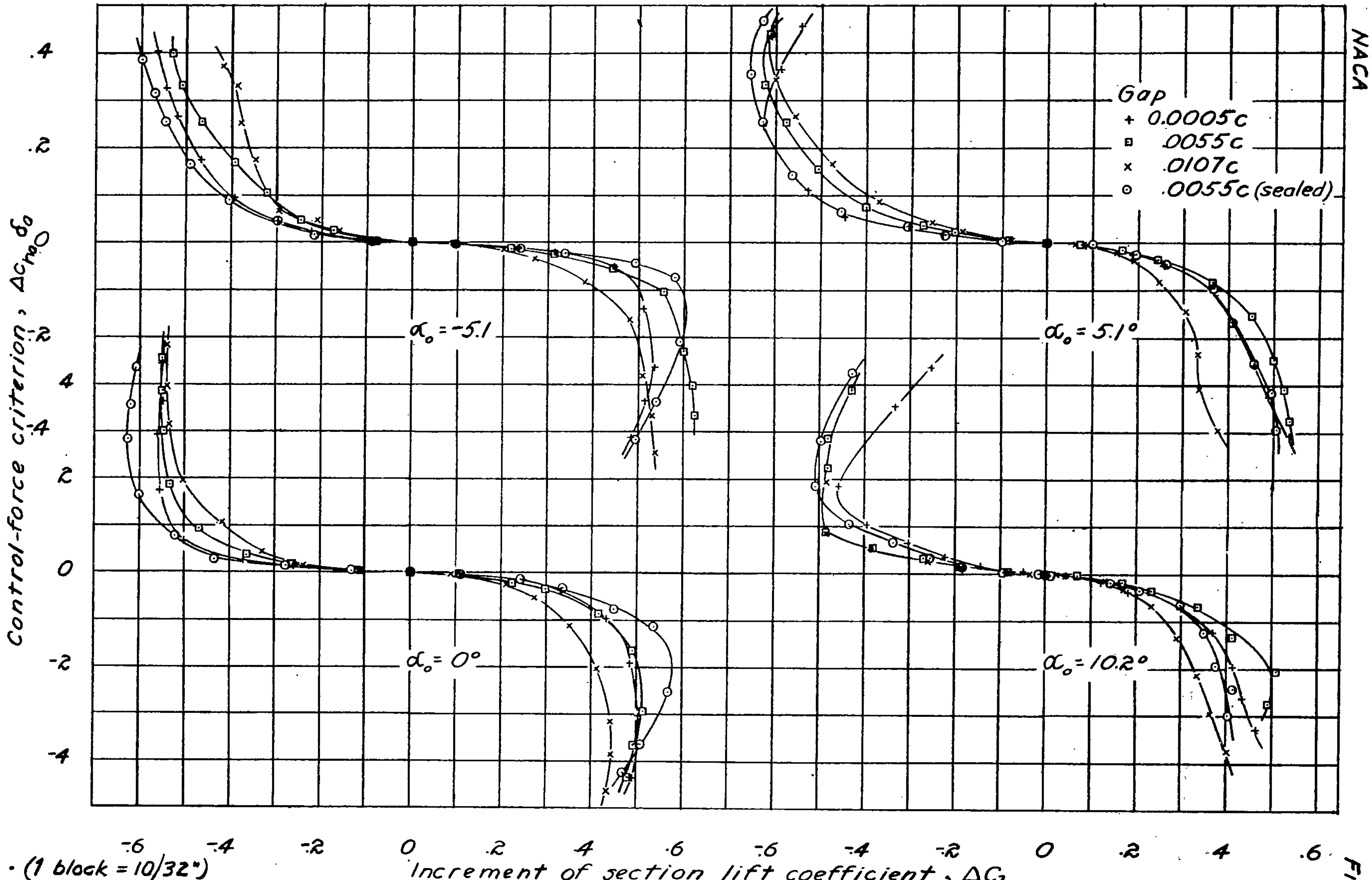

Figure 19. — Variation of control-force criterion with increment of section lift coefficient, showing effect of gap. Balance-nose radii = 0.020c; M = 0.417.

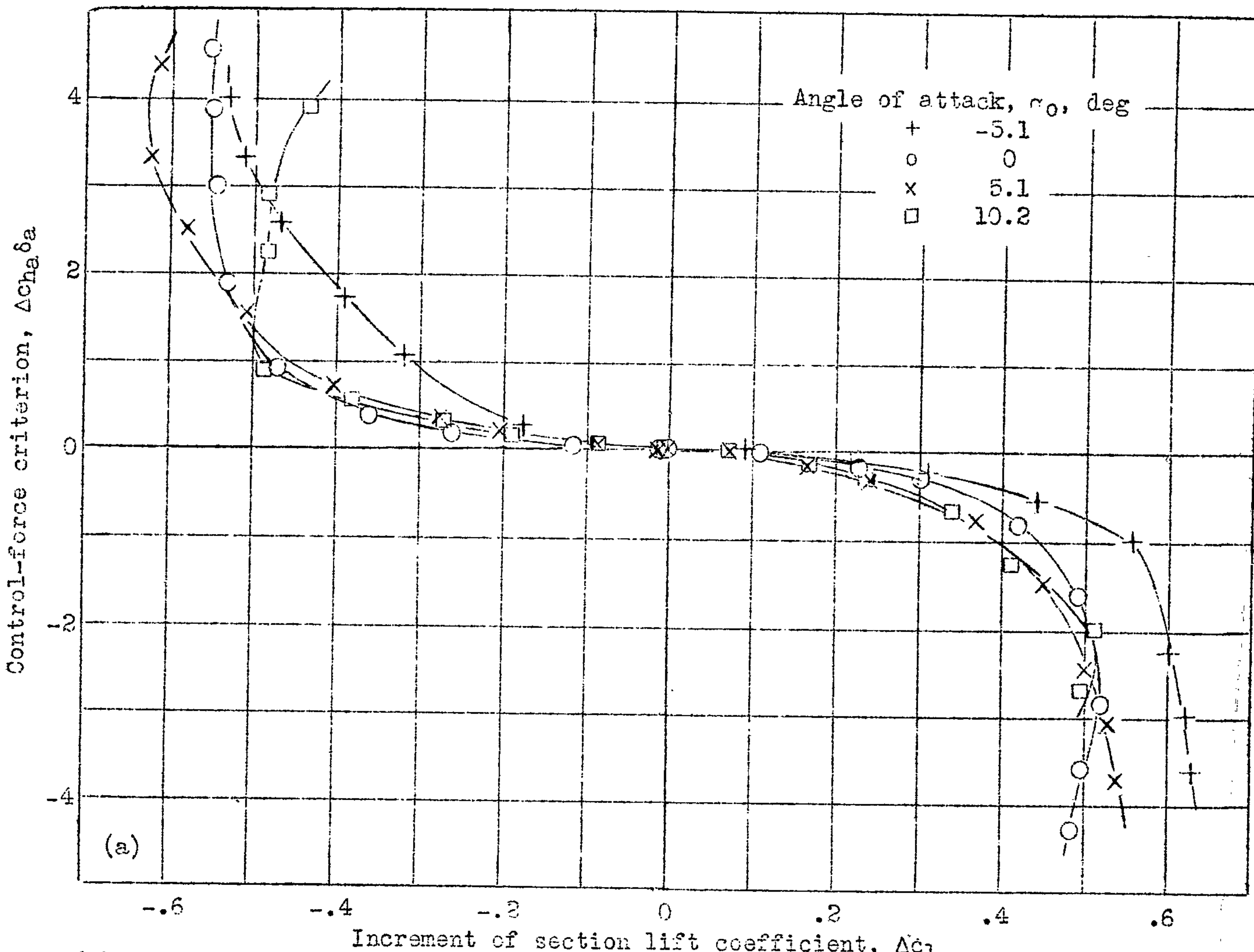

(a) M = .417

Figure 20(a,b).- Variation of control-force criterion with increment of section lift coefficient for the angle of attack range. Balance-nose radii = 0.02c; gap = 0.0055c.